# Ribonuclease P Catalysis Requires Mg 2+ Coordinated to the pro-R P Oxygen of the Scissile Bond †

**ARTICLE** *in* BIOCHEMISTRY · APRIL 1997

Impact Factor: 3.02 · DOI: 10.1021/bi9620464 · Source: PubMed



**3 AUTHORS**, INCLUDING:

Peter A Gegenheimer
University of Kansas
**32** PUBLICATIONS **1,551** CITATIONS

SEE PROFILE

# Ribonuclease P Catalysis Requires $Mg^{2+}$ Coordinated to the *pro-*$R_P$ Oxygen of the Scissile Bond†

Ying Chen,‡ Xinqiang Li,§ and Peter Gegenheimer*

Departments of Biochemistry and of Botany and Molecular Genetics Program, The University of Kansas, Lawrence, Kansas 66045-2106

*Received August 14, 1996; Revised Manuscript Received December 5, 1996*⊗

ABSTRACT: Ribonuclease P (RNase P) is an essential enzyme whose action produces the mature 5′ termini of all cellular and organellar transfer RNA molecules. In bacteria, the catalytic subunit of RNase P is an RNA molecule which by itself can bind substrate pre-tRNA, select and hydrolyze the correct phosphodiester bond, and release product tRNA. The simple requirements of the reaction—a monovalent cation such as $K^+$ or $NH_4^+$ and the divalent cation $Mg^{2+}$ (or $Mn^{2+}$)—have prompted proposals that all aspects of phosphodiester bond hydrolysis might be accomplished by one or more divalent metal cations coordinated to the enzyme or substrate. To precisely localize the ligands of catalytically-involved $Mg^{2+}$, we assayed cleavage by *Escherichia coli* RNase P RNA of pre-tRNA in which specific *pro-*$R_P$ phosphate oxygens were replaced with sulfur. RNase P cleavage was targeted to that bond, at or nearest to the normal cleavage site, at which $Mg^{2+}$ or $Mn^{2+}$ could be coordinated. Single-turnover kinetics demonstrated that the apparent rate constant for the hydrolysis event was determined quantitatively by the affinity of the divalent cation ($Mg^{2+}$ or $Mn^{2+}$) for the atom (O or S) at the *pro-*$R_P$ position of the scissile phosphodiester bond. We propose a model for pre-tRNA cleavage in which an essential $Mg^{2+}$ ion is coordinated directly to the *pro-*$R_P$ phosphate oxygen and indirectly to two other ligands near the scissile bond: the upstream ribose 2′-hydroxyl and the downstream purine N7. This catalytic $Mg^{2+}$ ion most likely positions and deprotonates a water molecule for in-line nucleophilic attack on the scissile bond phosphorus.

All naturally-occurring transfer RNAs are generated from precursor transcripts containing extraneous stretches of nucleotides which must be removed to produce functional tRNAs. Ribonuclease P (RNase P) is the endonuclease which catalyzes 5′-maturation of tRNA precursors [Altman & Smith, 1971; Robertson et al., 1972; reviewed by Altman (1989); Pace & Brown, 1995]. The substrate for the RNase P reaction is a 5′-extended precursor tRNA (pre-tRNA); the products are a mature tRNA with a 5′-terminal phosphoryl group and a 5′ leader with a 3′-hydroxyl terminus. RNase P from almost all species is a ribonucleoprotein containing an essential RNA subunit 200−400 nucleotides (nt) long and one or more polypeptides which range in size from 120 amino acids in bacteria to almost 1000 amino acids in yeast nuclei and mitochondria [Stark et al., 1978; Gardiner & Pace, 1980; Zimmerly et al., 1993; Morales et al., 1992; reviewed by Brown and Pace (1992); Darr et al., 1992]. The RNA subunit of bacterial RNase Ps, such as those from *Escherichia coli* and *Bacillus subtilis*, can carry out 5′ processing of tRNA precursors in the absence of the protein subunit [Guerrier-Takada et al., 1983; reviewed by Smith and Pace (1990); Altman, 1989]. The RNA subunit alone is sufficient to bind substrate, hydrolyze the correct phosphodiester bond, and release products. The catalytic RNA subunit of RNase P from *E. coli* has received considerable attention for three reasons. First, and unlike other ribozymes, it behaves like a classical enzyme in the sense that it binds a free substrate and catalyzes multiple rounds of cleavage (Guerrier-Takada et al., 1983; Pace & Smith, 1990). Second, unlike other ribozymes, RNase P interacts with its substrate primarily through noncanonical hydrogen bonds and van der Waals forces rather than through canonical Watson−Crick pairing (Smith et al., 1992). Third, unlike all other characterized ribozymes, RNase P catalyzes a direct hydrolysis reaction rather than a transphosphorylation (Marsh & Pace, 1985; Smith & Pace, 1993).

The simple requirements of the RNase P RNA-only reaction—a monovalent cation such as $K^+$ or $NH_4^+$ and the divalent cation $Mg^{2+}$ (or $Mn^{2+}$) (Guerrier-Takada et al., 1986; Gardiner et al., 1985; Surratt et al., 1990; Smith et al., 1992)—have prompted proposals that all aspects of catalysis might be accomplished by one or more divalent metal cations coordinated to phosphodiester oxygens of the enzyme (Haydock & Allen, 1985). In addition, important ligands of any catalytic $Mg^{2+}$ are likely to be phosphodiester oxygens of the substrate itself. The most plausible reaction mechanism, illustrated in Figure 1, is a standard in-line dissociative ($S_N2$-like) attack of a hydroxide ion on the phosphate immediately 5′ to the mature tRNA domain of the substrate [see Fersht (1985), pp 236−238]. Hydrolysis results in breakage of the bond between phosphorus and O3′ (the 3′ oxygen of the upstream ribose) which becomes the leaving group. A key aspect to this reaction is that the hydroxide must be positioned apically to O3′ (Cedergren et al., 1987). That the nucleophile is a hydroxide ion, rather than water,

† Supported in part by grants to P.G. from the University of Kansas General Research Fund (No. 3453 and No. 3484) and the NSF (DMB 91-06364 and OSR 92-55223).

* To whom correspondence should be addressed.

‡ Current address: Department of Developmental Hematology, Amgen Inc., Mail Stop 99-1-A, 1840 DeHavilland Dr., Thousand Oaks, CA 91320-1789

§ Current address: University of California at San Diego, Clinical Science Bldg. 410, 9500 Gilman Dr., La Jolla, CA 92093.

⊗ Abstract published in *Advance ACS Abstracts,* February 1, 1997.

S0006-2960(96)02046-6 CCC: $14.00 

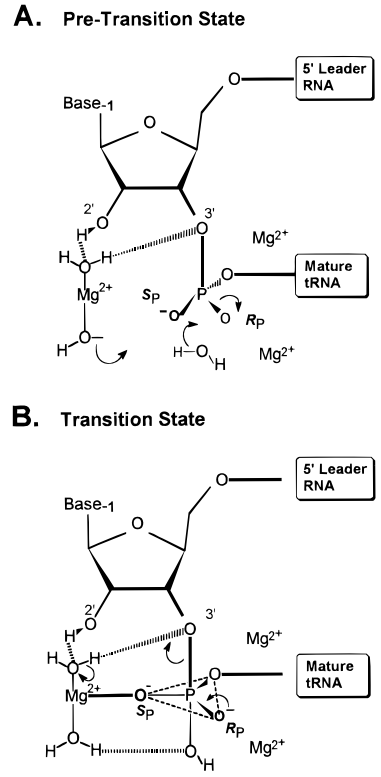


FIGURE 1: Model for RNase P catalysis based on models from Guerrier-Takada et al. (1986) and Smith and Pace (1993). (A) Pre-transition state. $[Mg(OH)]^+$, indirectly coordinated by the upstream 2′ OH, deprotonates a water molecule for apical nucleophilic attack on phosphorous. The phosphodiester backbone of the substrate is denoted by a heavy line. (B) Transition state. The *pro*-$S_P$ oxygen now coordinates the catalytic Mg hydrate. Two other $Mg^{2+}$ ions may stabilize the *pro*-$R_P$ oxygen and O3′ as the O3′−P bond is broken.

Scheme 1

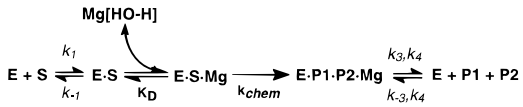


was inferred because the hydrolysis rate constant increases linearly with increasing $[OH^-]$ (Smith & Pace, 1993). Catalysis by the RNA subunit of *E. coli* RNase P absolutely requires divalent metal ions: hydrolysis proceeds optimally in the presence of $Mg^{2+}$ or $Mn^{2+}$ and weakly in the presence of $Ca^{2+}$ (Smith et al., 1992). Known catalytic roles for divalent metal cations include (i) facilitating the deprotonation of coordinated water molecules to provide hydroxide ions at neutral pH, (ii) polarizing a nonbridging phosphoryl oxygen to increase the electropositivity of phosphorus, and (iii) coordinating nonbridging phosphate oxygens to stabilize the pentacovalent transition state [see Fersht (1985), pp 67−69; Burgess, 1988; Pan et al., 1993]. In addition, a bound $Mg^{2+}$ ion in close proximity to the reactive phosphoryl could, by coordinating the attacking hydroxide, orient it properly to facilitate the reaction [see Beese and Steitz (1993)].

The RNase P hydrolysis reaction scheme can be presented in a simplified form (Scheme 1) where S represents pre-tRNA, P1 denotes the 5′ leader product ($k_3$, $k_{-3}$), and P2 denotes the mature tRNA ($k_4$, $k_{-4}$) [see Beebe and Fierke (1994)]. It is likely, as will be discussed, that either hydrated $Mg^{2+}$ or $[Mg(OH)]^+$ is the actual species which binds substrate. A proton and a hydroxyl ion equivalent to the magnesium-bound water are incorporated into the products. In this scheme, $k_{chem}$ is the first-order rate constant for the hydrolysis step. The experimentally-determined rate constant $k_{obs}$ measures the reaction steps from $Mg^{2+}$ binding through breakage of the scissile bond.

*Involvement of Metals in the RNase P Reaction.* The role of $Mg^{2+}$ in the RNase P reaction is both structural and catalytic. At low concentrations of monovalent cation, $Mg^{2+}$ can act to facilitate folding and charge neutralization of the RNase P RNA (Smith et al., 1992). Moreover, in the absence of monovalent cation, *B. subtilis* RNase P RNA assumes its mature conformation at about 6 mM $Mg^{2+}$, requiring cooperative binding of at least 3 $Mg^{2+}$ with a $[Mg^{2+}]_{0.5}$ of about 2−3 mM (Pan, 1995).

At saturating levels of monovalent cation (ca. 1 M $NH_4^+$, $K^+$, or $Na^+$), only moderate concentrations of $Mg^{2+}$, ca. 10 mM, are needed for optimal steady-state activity (defined by $k_{cat}/K_M$) of *E. coli* RNase P RNA (Smith et al., 1992). Haydock & Allen (1985) first proposed a model in which RNase P RNA might catalyze phosphodiester hydrolysis by providing a specific binding site for $Mg^{2+}$. In this model, a variant of which is illustrated in Figure 1, one of the equatorial ligands of the catalytic $Mg^{2+}$ is a nonbridging phosphodiester oxygen of the RNase P RNA. An inner-sphere $OH^-$, as the "lower" axial ligand to $Mg^{2+}$, acts as a general base, deprotonating an outer-sphere $H_2O$ to provide the nucleophilic $OH^-$ which attacks the scissile phosphodiester opposite to O3′. In the transition state, this $Mg^{2+}$ also provides equatorial coordination to the *pro*-$S_P$ nonbridging oxygen of the scissile bond. Finally, an inner-sphere water as the "upper" axial ligand serves as a general acid, donating a proton to the leaving O3′.

Smith and Pace (1993) elaborated on this model, providing evidence that a water axially liganded to a catalytically-required $Mg^{2+}$ ion was further hydrogen bonded to the 2′-OH of the upstream nucleotide (pre-tRNA position −1). This binding is also illustrated in Figure 1. Those experiments also indicated that at least two more $Mg^{2+}$ ions are required for catalysis. Between 1 and 10−20 mM $Mg^{2+}$, the rate constant for hydrolysis increases cooperatively with increasing $[Mg^{2+}]$; the Hill coefficient is 3 (Smith & Pace, 1993), suggesting that at least 3 $Mg^{2+}$ ions bind together to effect catalysis. [Above ca. 15 mM, $Mg^{2+}$ binding is almost noncooperative, with a Hill coefficient of 1.4; see Figure 6 of Smith and Pace (1993).] In those experiments, the apparent $[Mg^{2+}]_{0.5}$ was ca. 1−6 $\mu$M, comparable to the $K_D$ for previously-described "tight" binding sites in tRNAs [reviewed in Pan et al. (1993)]. When the 2′-hydroxyl of the nucleotide 5′ to the cleavage site was removed, the cooperativity of $Mg^{2+}$ binding was reduced to 2 with a $[Mg^{2+}]_{0.5}$ of 6 mM (Smith & Pace, 1993) or about the $K_D$ for nonspecific binding of $Mg^{2+}$ to tRNA (Pan et al., 1993). These data strongly implicate the upstream 2′-OH in forming a specific binding site for a single catalytically-involved $Mg^{2+}$ ion. Independent investigations have confirmed the participation of multiple Mg ions in the reaction. Hardt et al. (1993) determined that binding of two $Mg^{2+}$ ions accompanied formation of the E·S complex during equilibrium binding experiments. Beebe et al. (1996) also identified two $Mg^{2+}$ binding sites (or classes of sites) whose occupancy stabilizes the E·S or E·P complex and additionally a third site whose occupancy is required for phosphodiester bond hydrolysis.

*The Two-Metal−Ion Mechanism and Its Implications.* A plausible model for metal−ion-dependent hydrolysis and phosphoryltransfer reactions catalyzed by RNAs was devel-

oped by Steitz and Steitz (1993) based on the crystal structure of protein metalloenzyme phosphoryltransferases/hydrolases such as alkaline phosphatase (Kim & Wyckoff, 1991), phospholipase C (Hough et al., 1989), P1 nuclease (Volbeda et al., 1991), and the 3′ → 5′ proofreading exonuclease domain of *E. coli* DNA polymerase I ("Pol I Exo"; Beese & Steitz, 1991). The crystal structure of Pol I Exo reveals two bound divalent metal cations ($Zn^{2+}$ in the crystal; $Mg^{2+}$ or $Zn^{2+}$ in vivo). The first metal, occupying a location designated site A, is positioned to coordinate the *pro*-$S_P$ oxygen of the scissile phosphodiester as well as the attacking nucleophilic water or hydroxide; the crucial deprotonation of water is accomplished by $Mg^{2+}$−A acting as a Lewis acid. The second metal, occupying site B, could bond to the *pro*-$S_P$ oxygen as well as to O3′, thus stabilizing the geometry of the transition state and neutralizing the developing charge on the leaving group. Each ion is further fixed in position by inner- or outer-sphere coordination to three carboxylate oxygens of acidic amino acids. In the mechanism proposed for Pol I Exo, the attacking water is also positioned by hydrogen bonding to the hydroxyl of Tyr497. The hydroxyl of Tyr497 occupies a spatial position which we refer to as site C.

As this active-site structure depends solely upon appropriately-positioned oxygens to provide ligands to the catalytic magnesiums and the attacking hydroxyl, it can easily be extended to cover catalysis by RNA enzymes (Steitz & Steitz, 1993). RNA molecules provide a high density of metal ligands, direct or indirect, in the form of ribose hydroxyls, phosphodiester oxygens, and ring nitrogens and oxygens. In an RNA enzyme, divalent cations, positioned as in Pol I Exo or alkaline phosphatase, could accomplish most or all of the chemistry and transition-state stabilization obtained by the protein enzymes. As the major role of catalytic amino acid side chains in these reactions (at least in Pol I Exo) appears to be to provide ligands for the metals or the substrate oxygens, these amino acids could also be replaced by divalent cations or by nucleic acid constituents.

*Thio Effects in Ribozyme Reactions.* Previous research has shown that *pro*-$R_P$ phosphorothioate substitutions in oligonucleotide substrates have a notable rate effect in ribozyme-catalyzed phosphodiester hydrolysis reactions. Some of these "thio effects" reflect intrinsic chemical reactivity of phosphorothioate (Herschlag et al., 1991), whereas others result from reduced divalent cation binding (Dahm & Uhlenbeck, 1991; Piccirilli et al., 1993; Christian & Yarus, 1993). As a "hard" metal, $Mg^{2+}$ binds substantially better to "hard" ligands such as oxygen than to "soft" ligands such as sulfur (Jaffe & Cohn, 1978, 1979; Pecoraro et al., 1984; Pan et al., 1993). On the other hand, $Mn^{2+}$ is a softer metal which discriminates against sulfur less strongly than does $Mg^{2+}$. The magnitude of this effect was calculated by Pecoraro et al. (1984) for $Mg^{2+}$ or $Mn^{2+}$ coordination by the $\beta$-phosphoryl of ATP. Replacement of the *pro*-$R_P$ $\beta$-oxygen by sulfur decreased $K_A$ for $Mg^{2+}$ by 31000-fold, whereas $K_A$ for $Mn^{2+}$ was reduced only by about 175-fold. In other words, $Mn^{2+}$ binds S about 177-fold (31000/175) better than does $Mg^{2+}$. Hence, a reaction which is inhibited by thiosubstitution of an essential oxygen can be restored or "rescued" by concomitant replacement of $Mg^{2+}$ with $Mn^{2+}$.

Other differences between phosphate and phosphorothioate are the greater length of the P−S bond, the apparent redistribution of negative charge to the sulfur (Frey & Sammons, 1985), and the inability of sulfur to accept hydrogen bonds. Consistent with this, a second class of phosphodiester interactions has been characterized for which phosphorothioate substitution decreases $k_{chem}$ by a magnitude—up to 1000−3000-fold—comparable to loss of coordination but for which $Mn^{2+}$ rescue is not observed. Such interactions have been characterized at the *pro*-$S_P$ oxygen of the scissile bond in the first step of the *Tetrahymena thermophila* group I intron self-splicing reaction [Rajagopal et al., 1989; the *pro*-$R_P$ oxygen in the reverse reaction is the *pro*-$S_P$ position in the forward reaction, Herschlag et al. (1991)] and at several positions in the *E. coli* RNase P RNA (Harris & Pace, 1995; Hardt et al., 1995). These observations are consistent with indirect or outer-sphere coordination of a ligand such as hydrated $Mg^{2+}$; that is, hydrogen bonding between inner-sphere water and phosphate oxygen [e.g. Dunaway-Mariano and Cleland (1980)]. Such inhibition could also result from failure to accept H-bonds from other ligands or from steric or electronic exclusion of these ligands from their binding site(s).

In the present work, we examined the role of $Mg^{2+}$ or $Mn^{2+}$ in phosphodiester hydrolysis by replacing specific *pro*-$R_P$ oxygens with sulfur in the substrate precursor tRNA. We identified the scissile bond in precursor $tRNA^{Phe}$ as the sole position where *pro*-$R_P$ phosphorothioate substitution inhibits cleavage, and we took advantage of the differential affinity of $Mg^{2+}$ and $Mn^{2+}$ for oxygen versus sulfur to demonstrate that at least one catalytically-essential $Mg^{2+}$ ion is coordinated directly by the *pro*-$R_P$ nonbridging oxygen of the scissile bond.

## EXPERIMENTAL PROCEDURES

*Reagents.* All chemicals were of reagent grade or higher; $NH_4Cl$, $MgCl_2$, and $MnCl_2$ were ultrapure (Aldrich; 99.99−99.995%). All solutions were prepared in organic-free water (Barnstead Nano-Pure II, 0.2 $\mu$m filter) and were either autoclaved or prepared with sterile water. $MgCl_2$ and $MnCl_2$ were prepared as 1.0 M stocks in 50 mM MES−KOH[1] buffer, pH 6.0, and stored at −20 °C. DTT stock solutions (1.0 M or 50 mM) were stored at −20 °C. Oligodeoxynucleotides were synthesized and desalted by Macromolecular Resources (Colorado State University) and were used without further purification.

*Plasmid Constructs.* Plasmid p67YF0, obtained from O. C. Uhlenbeck, carries a synthetic gene, "YF0", encoding mature $tRNA^{Phe}$ with a 3′-terminal CCA sequence behind a phage T7 promoter (Sampson et al., 1988). Plasmid pBSYF0 was constructed by inserting the YF0 gene and T7 promoter downstream of the phage T3 promoter in plasmid pBS(−) (Stratagene). In vitro transcription of this plasmid with T3 RNA polymerase yields pre-$tRNA^{Phe}$ plus a 5′ leader sequence consisting of T7 promoter sequences and a mature 3′-terminal $CCA_{OH}$ sequence. Plasmid pBSYF0-A1U72 has a sequence identical to plasmid pBSYF0 except that base G1 (with respect to the start of mature $tRNA^{Phe}$) was changed to A and the complementary base C72 was changed to U as described below. Plasmid pDW27, gener-

[1] Abbreviations: NMPαS, α-phosphorothioate nucleoside [nucleoside 5′-*O*-(1-thiomonophosphate)]; NTPαS, nucleoside 5′-*O*-(1-thiotriphosphate); p(S)Gp, guanosine 5′-*O*-(1-thiomonophosphate), 3′-monophosphate; pA, adenosine 5′-monophosphate; DTT, dithiothreitol; MES, 2-(*N*-morpholino)ethanesulfonic acid; PEI, poly(ethylene)imine; TE, Tris/EDTA buffer.

ously provided by D. Waugh and N. R. Pace, contains a DNA fragment encoding the RNA component of *E. coli* RNase P transcribed from a phage T7 promoter (Waugh et al., 1989).

*Gene Construction.* To construct pBSYF0-$A_1U_{72}$, the YF0 gene in pBS(−)YF0 was amplified using two synthetic primers: left, YF0-G1A.L2 (5′-GCA TGC CTG CAG TAA TAC GAC TCA ATA TAa CGG ATT T, position −18 to +8) and right, YF0-C72U.R4 (5′-ATC CTC TAG AGG ATC CTG GTa CGA ATT CTG TGG AT, position +92 to +58). The lowercase letters represent the changes at positions +1 and +72 which replaced the first base pair G:C of the acceptor stem of tRNA with A:U. The amplification reaction (100 $\mu$L) contained 20 ng (67 nM) plasmid, 2.5 mM each dNTP, 1 mM each primer, 25 units/mL *Taq* DNA polymerase (Perkin-Elmer Cetus), 50 mM KCl, 10 mM Tris-HCl (pH 8.3), and 1.5 mM $MgCl_2$. The gene was amplified for 25 cycles of 94 °C (1.5 min)/65 °C (1.0 min)/72 °C (1.0 min). The amplified DNA was purified by phenol−chloroform extraction and was subcloned into plasmid pBS(−) as described in Oommen et al. (1992) except that vector and insert were electroeluted from agarose gels. The base changes were confirmed by manual sequencing with oxidized T7 DNA polymerase (Sequenase 1.0, US Biochemicals).

*Plasmid DNA Preparation.* Plasmid DNA was prepared and stored following the large-scale preparation protocol described in Oommen et al. (1992) except that cells were lysed with alkaline Na dodecyl sulfate (Sambrook et al., 1989) and sterile TE buffer was used in the chromatographic separation of plasmid DNA from RNA. Prior to transcription, pBS(−)YF0 and p67YF0 plasmids were digested to completion with *Bst*N1, and pDW27 with *Sna*B1. The DNA fragments were again purified by phenol−chloroform extraction, concentrated by ethanol precipitation, and resuspended in sterile distilled water or TE buffer (pH 8.0).

*In Vitro Transcription.* The phage T3 RNA polymerase transcript of *Bst*N1-digested pBSYF0 is called pre-$tRNA^{Phe}$ or pre-$G_1$Phe. The T3 polymerase transcription product of *Bst*N1-digested pBSYF0-$A_1U_{72}$ is referred to as pre-$A_1$Phe. When T7 RNA polymerase transcription of *Bst*N1-digested plasmid p67YF0 is primed with [$^{32}$P]pApG, the resultant pre-$tRNA^{Phe}$ transcript contains [$^{32}$P]pA ("*pA") as its 5′ leader and is designated *pA-tRNA. The catalytic RNA component of *E. coli* RNase P is transcribed by T7 polymerase from plasmid pDW27 linearized with *Sna*B1.

For preparation of labeled substrate, 100 $\mu$L transcription reaction mixtures contained 40 mM Hepes (pH 8.0), 20 mM $MgCl_2$, 25 mM KCl, 5 or 10 mM dithiothreitol (DTT), 70 $\mu$g/mL acetylated bovine serum albumin, 2 mM each ribonucleoside triphosphate (rNTP), 50−100 $\mu$g/mL linear DNA, 100−200 $\mu$Ci [$\alpha$-$^{32}$P]rNTP(s), 10−20 units/mL RNase inhibitor (InhibitAce, 5′ → 3′ Inc.), and 1000 units/mL RNA polymerase from phage T3 (Promega) or T7 (USB or Promega). Incubation was for 2−4 h at 37 °C. Substrates for kinetic study were transcribed to achieve high specific activity, with one of the rNTPs reduced to 0.1−0.2 mM and its corresponding [$\alpha$-$^{32}$P]rNTP as the only radioactive label. Transcripts fully substituted with phosphorothioate 5′ to a given nucleotide were produced by in vitro transcription in the presence of the corresponding ribonucleoside 5′-*O*-(1-thiotriphosphate) (rNTP$\alpha$S) (New England Nuclear) and each of the three other unsubstituted rNTPs, all at 2 mM. The RNA component of *E. coli* RNase P was synthesized using an Ampliscribe T7 Kit (Epicentre Technologies), and the amount of [$\alpha$-$^{32}$P]rNTP was decreased to about 1 $\mu$Ci per 100-$\mu$L reaction.

Dinucleotide-primed transcription was accomplished as follows: Adenylyl(3′−5′)guanosine (ApG) (Sigma) was labeled at its 5′ end with [$\gamma$-$^{32}$P]ATP and T4 polynucleotide kinase in 20 $\mu$L containing 3 mM ApG, 20 mM Na−$PO_4$ (pH 7.5), 10 mM $MgCl_2$, 250 $\mu$Ci [$\gamma$-$^{32}$P]ATP (NEN), and 1 unit of T4 polynucleotide kinase (Promega). The mixture was incubated at 37 °C for 30 min. A 10 $\mu$L portion was used directly in a 60 $\mu$L in vitro transcription reaction containing 5 $\mu$g of p67YF0/*Bst*N1 DNA, 20 mM Na−$PO_4$ (pH 7.5), 10 mM $MgCl_2$, 10 mM DTT, 1.5 mM GTP or GTP$\alpha$S (as required), 1.5 mM each of the other three rNTPs, and 1000 units/mL T7 RNA polymerase.

Transcription reactions were terminated by addition of 0.5 vol 10 M urea/3× loading dye (Wang et al., 1988) and heating for 5 min at 65 °C. Products were purified on denaturing polyacrylamide gels, detected by autoradiography, and eluted by diffusion all as described previously (Wang et al., 1988). RNAs were precipitated with ethanol, resuspended in distilled water, and stored at −20 °C.

*Processing Reactions and Product Analysis.* The reaction conditions for RNase P RNA subunit includes either 50 mM Tris-HCl (pH 8.0) or 50 mM MES−KOH (pH 6.0), 1.0 or 0.1 M $NH_4Cl$ (99.99% pure, Aldrich Chemical Co.), and 5−100 mM $MgCl_2$ (99.995%, Aldrich) or 2−60 mM $MnCl_2$ (99.99%, Aldrich). Most reactions contained 0.1−0.5% Na dodecyl sulfate. Some reactions with phosphorothioate-containing RNA also included 10 mM DTT, although comparable results were obtained with or without reductant. The amount of substrate and enzyme added is indicated for each individual figure. Most steady-state reactions were terminated by heating with 0.5 volume of urea/dye mix, as above; a few were stopped by addition of 1 $\mu$g of nuclease-free glycogen, EDTA to 20 mM, and precipitation with 3 volumes of 95% EtOH overnight at −20 °C. The pellet was collected by centrifugation, resuspended in 10 $\mu$L of TE buffer, and denatured as above. Reaction products were separated by electrophoresis on 10% polyacrylamide/7 M urea gels. For processing of [5′-$^{32}$P]pApG-primed pre-tRNA, the released mononucleotide *pA was resolved by chromatography on 10 cm high PEI−cellulose thin-layer plates (MN Cell 300/UV254 from Brinkmann, prewashed with absolute methanol, dried, and prerun with water). The plates were developed with 0.5 M formic acid to 5 cm, air dried, and developed to the top with 0.15 M Li−formate (pH 3.0) (Volckaert & Fiers, 1977). This system cleanly separates pA from $P_i$ and from all nucleoside bisphosphates. After air drying, the plates were visualized by exposure to X-ray film.

*5′ End Analysis.* Gel-purified and ethanol-precipitated tRNAs were resuspended in 5 $\mu$L of carrier RNA (1 mg/mL in $H_2O$), transferred to a sheet of parafilm, and mixed with 5 $\mu$L of RNase T2 (1 unit/$\mu$L in 200 mM $NH_4OAc$). RNA remaining in each tube was recovered with 1 $\mu$L of distilled water, transferred to another piece of parafilm, and mixed with 5 $\mu$L of P1 nuclease (1 mg/mL in 20 mM $NH_4OAc$). Both RNase T2 and P1 nuclease reactions were incubated in sealed capillaries for 5−6 h at 50 °C. The digest was then spotted onto a prewashed PEI−cellulose thin-layer plate. Unlabeled internal markers pAp and pGp, ~5 $\mu$g each, were also applied to the plate in every sample. After the applied samples had dried (and the origin was optionally washed 5 min in MeOH and dried), the plate was developed

in 1.6 M LiCl. After development, the dried plate was either washed in MeOH for 5 min or wrapped in plastic wrap. The plate was marked with luminescent paint and exposed to Kodak XAR film with an intensifying screen at −70 °C.

*Determination of $k_{obs}$.* Cleavage reactions were as described above, using pH 6.0 buffer except where stated, the divalent metal concentrations indicated in the text or figure legends, and incubation times between 1 and 3 half-lives. In each reaction, 0.5−2 nM substrate and 50−600 nM RNase P RNA subunit were used. The concentration of enzyme required for saturation was first determined at each $M^{2+}$ concentration being tested by titrating substrate with increasing RNase P RNA (e.g. 57, 190, and 570 nM) until $k_{obs}$ reached a plateau. Substrate and enzyme were separately incubated in processing buffer at 37 °C for 10−30 min to promote proper folding. Reactions were initiated by mixing enzyme and substrate. Ten microliter aliquots were withdrawn at appropriate intervals, and reactions were quenched in an equal volume of 10 M urea/loading dye mix at 65 °C for 3−5 min. Uncleaved precursor and mature tRNA were separated by polyacrylamide gel electrophoresis, detected by autoradiography, and quantified by Cerenkov counting of excised gel slices in water. The radioactivity in each gel slice was corrected for in-lane background by subtracting the cpm of a similar-sized gel slice taken just below the substrate slice. To correct for nonspecific hydrolysis of the $^{32}$P-labeled enzyme RNA in reactions conducted for more than a few hours, a separate enzyme-only blank reaction was performed for every experimental time, and the cpm of substrate and product in each reaction was corrected for the cpm in the same region of the parallel reaction lacking substrate.

The observed hydrolysis rate constant, $k_{obs}$, was determined from plots of the percentage of substrate remaining versus time ($F_S = S_t/[S_t + P_t]$, where $F_S$ is the fraction of substrate remaining at time $t$, and $S_t$ and $P_t$ are the cpm of substrate or product at time $t$). The data were fitted by the single-exponential decay equation with the program Enzfitter (Biosoft) using Marquardt−Levenberg least-squares nonlinear regression and robust statistical weighting. Data sets which had an apparent lag phase prior to cleavage were fit by an equation describing sequential pseudo-first-order binding followed by first-order cleavage, $F_S = \{F_0/(k_2 - k_1E)\}\{k_2e^{-k1Et} - k_1Ee^{-k_2t}\}$, where E is [enzyme] and $k_1E$ is then the apparent first-order association rate constant [Beebe & Fierke, 1994; see Fersht (1985), pp 133−134; Cox, 1994; Gutfreund, 1995, pp 110−114].

*Computational. Compilation of tRNA 5′ Terminal Bases.* The tRNA sequence compilation (Steinberg et al., 1993) was obtained from ftp.embl-heidelberg.de/pub/databases/trna. Data fields and sequence segments were parsed and extracted into a flat-file database. RNA sequences with modified bases were converted to the corresponding unmodified DNA sequences, and for each isoacceptor the first RNA sequence which (except for the 3′-terminal CCA) duplicated a DNA sequence entry was eliminated. All sequences which initiated with base 0 ($tRNA^{His}$) or base +2 were excluded, and the first base of the remaining sequences was cross-tabulated by sequence and kingdom. The modified database, in several formats, is available electronically from http://RNAworld.bio.ukans.edu/transfer/RNaseP/ or by anonymous ftp from RNAworld.bio.ukans.edu.

*Molecular Model Building.* A physical model of the dinucleotide adenylyl guanosine was first constructed using a plastic straw-type kit (Minit system, Cochranes of Oxford Ltd., Leafield, Oxford OX8 5NT, U.K.). A hydrated $Mg^{2+}$ ion was built from a hexavalent Fe atom with five $OH_2$ groups positioned at the consensus Mg−O distance of 2.0 Å [e.g. Holbrook et al. (1977)]. A pentacovalent atom center, built by adding two apical connectors to a 120° trivalent carbon center, was substituted for the phosphorus. To this transition state center, O5′ was attached coplanar to the nonbridging oxygens and an $OH^-$ was attached apically to O3′. The $Mg(OH_2)_5$ was attached to the *pro-*$R_P$ oxygen of the phosphodiester, and the model was then rotated by hand to permit replacement of one Mg-bound water with the $OH^-$. To test whether another Mg-bound water could accept an H-bond from the upstream ribose 2′-hydroxyl, as proposed by Smith and Pace (1993), the model was rotated into the appropriate configuration. At this point, it became apparent that rotation about the P−O5′ and C1−N9 bonds would position the guanine ring underneath the hydrated $Mg^{2+}$, such that Gua-N7 could accept a standard-geometry H-bond from $Mg(OH_2)_5$.

To confirm the feasibility of this structure, it was generated computationally starting with the refined 3-dimensional coordinates of yeast $tRNA^{Phe}$ (PDB entry 6TNA: Sussman et al., 1978). The A-helical dinucleotide A29−G30 was chosen as a model of the scissile bond A(−1)−G1 because G1 is at the end of the A-helical acceptor stem and A(−1) can stack on G1. The coordinates for nucleotides 29 and 30, a fully-hydrated $Mg^{2+}$, and $H_2O$ were extracted from the PDB file, and explicit hydrogens were added with Sybyl 6.0 (Tripos Associates). Further manipulations were performed with the PC-based software Molecular Images (D. McRee, distributed by Molecular Images Software, San Diego, CA). The resultant computer model is similar to the physical model except for the computer model's poorer H-bond angle between $Mg(OH_2)_5$ and Gua-N7. Nonetheless, the C8−N7−OB angle and C6−C5−N7−OB dihedral are not too dissimilar from those found at G20 of the $tRNA^{Phe}$ structure 6TNA. Initial attempts to improve or confirm this model by energy minimization in Sybyl were unsuccessful because of the inability of the software to correctly model coordinate bonds. All relevant data files in PDB format, as well as images generated therefrom, are available electronically as above.

## RESULTS

*$R_P$-Phosphorothioate Substitution Only at the Scissile Bond Inhibits Cleavage by the RNA Subunit of E. coli RNase P.* The RNA subunit of *E. coli* RNase P recognizes substrate pre-tRNA in a structure- rather than a sequence-specific fashion and interacts with pre-tRNA via hydrogen bonding and van der Waals interactions rather than by electrostatic interactions (Smith et al., 1992). Our initial objective was to locate pre-tRNA phosphodiester bond phosphates which might interact directly with RNase P. Since the electronic configuration of phosphorothioate differs from that of phosphate (Frey & Sammons, 1985) and sulfur is not an H-bond acceptor, we reasoned that replacement of phosphodiester nonbridging oxygens with sulfur might alter the ability of RNase P to bind substrate. For example, replacement of phosphodiesters by phosphorothiodiesters at certain positions in bacteriophage R17 mRNA reduced binding of coat protein to its binding site (Milligan & Uhlenbeck, 1989). More dramatically, replacement of a phosphoryl oxygen by sulfur will also virtually abolish coordination of $Mg^{2+}$ ions

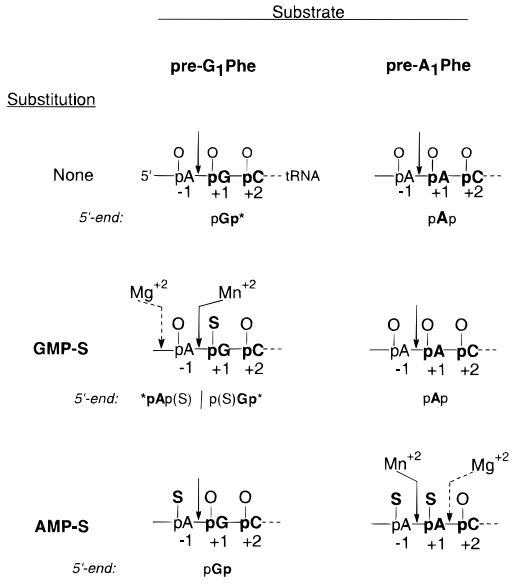


FIGURE 2: Sequence surrounding the scissile bond of pre-tRNA$^{Phe}$ variants. Position +1 is the 5′-end of the mature tRNA domain. Wild-type yeast pre-tRNA$^{Phe}$ is called pre-$G_1$Phe; the variant with A at position +1 is called pre-$A_1$Phe. Arrows indicate the major positions of hydrolysis by the RNase P RNA subunit under steady-state conditions in buffer containing either $Mg^{2+}$ (10−20 mM) or $Mn^{2+}$ (2−20 mM) as described in the text. Unless specified, both $Mg^{2+}$ and $Mn^{2+}$ promote hydrolysis of the same bond. Beneath each sequence is given the mononucleoside bisphosphate released by RNase T1 digestion from the 5′ end of the processed tRNA and detected by TLC analysis (this work; X. Li, Ph.D. Thesis, University of Kansas, 1992). Asterisks indicate $^{32}$P label, as explained in the text and legend to Figure 7.

to this oxygen. RNA polymerase stereoselectively incorporates $S_P$-nucleoside 5′-*O*-(1-thiotriphosphate)s (α-thio-nucleotides, referred to subsequently as NTPαS), with inversion of configuration, giving RNA transcripts containing $R_P$-nucleoside phosphorothioates [see Eckstein (1985)]. By placing phosphorothioates at various positions in precursor tRNA and processing these substrates with RNase P RNA, we could infer the location of *pro*-$R_P$ oxygens which are essential for enzyme·substrate binding or for $Mg^{2+}$ coordination. The substrate we used was a semisynthetic precursor to yeast tRNA$^{Phe}$, containing a 3′-mature $CCA_{OH}$ and a 43-nucleotide 5′ extension. The sequence surrounding the scissile bond is shown in Figure 2 (substrate pre-$G_1$Phe). RNase P cleaves the bond between $A_{-1}$ and $G_{+1}$ with respect to the 5′ terminus of mature tRNA.

By in vitro transcription, we synthesized four pre-tRNA$^{Phe}$ substrates, each of which included a 100% replacement of one nucleoside 5′-monophosphate (NMP) by the corresponding nucleoside 5′-monophosphorothioate (NMPαS). The substrates thus contained a sulfur at the nonbridging $R_P$ position of the phosphoryl 5′ to every adenosine (giving a transcript called pre-tRNA[AMPαS]), cytosine (pre-tRNA-[CMPαS]), guanosine (pre-tRNA[GMPαS]), or uridine (pre-tRNA[UMPαS]). These sulfur-containing substrates were processed to completion with RNase P RNA subunit in 1 M $NH_4Cl$ and 10 mM $MgCl_2$, conditions which are optimal for steady-state reaction (Smith et al., 1992). Figure 3 demonstrates that substrates pre-tRNA[AMPαS] (lane 4) and pre-tRNA[UMPαS] (lane 10) are cleaved to completion, as is the unsubstituted substrate (lane 2), and that pre-tRNA-[CMPαS] (lane 6) is also cleaved, though with a modestly reduced efficiency. (This effect is attributable to an increased $K_D$ of the pre-tRNA−enzyme complex (Hardt et al., 1995).)

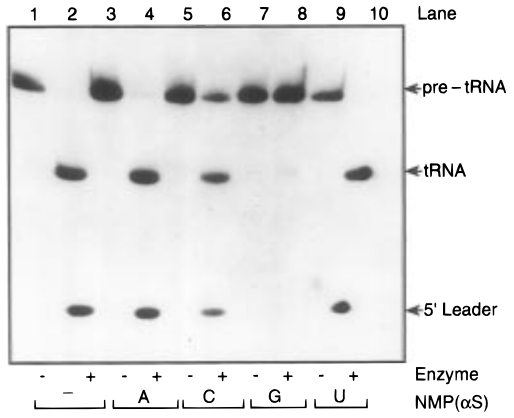


FIGURE 3: Processing of thio-substituted yeast pre-tRNA$^{Phe}$ by *E. coli* RNase P RNA. Yeast pre-tRNA$^{Phe}$ (pre-$G_1$Phe) was synthesized either with all-oxygen-containing nucleotides (lanes 1 and 2) or containing 100% substitution with AMPαS (lanes 3 and 4), CMPαS (lanes 5 and 6), GMPαS (lanes 7 and 8), or UMPαS (lanes 9 and 10). Substrate RNA (45−70 nM) was incubated with 50 nM *E. coli* RNase P RNA subunit in 20 μL of 50 mM Tris-HCl (pH 8.0), 1 M $NH_4Cl$, and 10 mM $MgCl_2$ at 37 °C for 135 min. Products were separated by electrophoresis on a 10% polyacrylamide gel containing 7 M urea, an autoradiograph of which is shown. (Lane 10 is skewed to the left.)

Surprisingly, as shown in lane 8 of Figure 3, under identical conditions RNase P RNA subunit completely failed to process pre-tRNA[GMPαS]. RNase P RNA activity is thus significantly inhibited by thio substitution at one or more of the phosphodiester bonds 5′ to guanosines in the substrate. This result was unexpected, but proved intriguing: Since the scissile bond itself lies 5′ to a guanosine, the GMPαS-dependent inhibition might result not from failure of enzyme to bind substrate but from failure of a catalytically-required $Mg^{2+}$ to coordinate the scissile phosphodiester.

To determine whether thio substitution at the scissile bond rather than at other positions was responsible for inhibition of RNase P activity, we compared processing of the wild-type pre-tRNA$^{Phe}$, referred to subsequently as pre-$G_1$Phe, with that of a variant, designated pre-$A_1$Phe, in which base $G_{+1}$ was changed to A (and the complementary $C_{72}$ to U). The sequence surrounding the scissile bond of these substrates and the positions of thio substitutions are shown in Figure 2. If the *pro*-$R_P$ phosphate oxygen 5′ to the scissile bond is the only oxygen necessary for cleavage, pre-$G_1$Phe[GMPαS] will not be cleaved but pre-$A_1$Phe[GMPαS] will be, whereas pre-$G_1$Phe[AMPαS] will be cleaved but pre-$A_1$Phe[AMPαS] will not be. Figure 4 presents the results of an experiment in which substrates pre-$G_1$Phe and pre-$A_1$Phe were processed to completion with *E. coli* RNase P RNA subunit in 10 mM $MgCl_2$. As expected, RNase P RNA could not cleave pre-$G_1$Phe[GMPαS] (shown in lane 1). However, pre-$A_1$Phe-[GMPαS] was cleaved (lane 2). Furthermore, pre-$G_1$Phe[AMPαS] was an efficient substrate (lane 4), whereas pre-$A_1$Phe[AMPαS] was essentially inactive (lane 5).

To confirm that phosphorothioates at positions other than the scissile bond had no effect upon RNase P action, we prepared another pre-tRNA$^{Phe}$ substrate by priming in vitro transcription with the dinucleotide [5′-$^{32}$P]pApG, giving a pre-tRNA called *pA-tRNA (* indicates the $^{32}$P label) whose 5′ leader is [5′-$^{32}$P]AMP and whose scissile bond is a conventional phosphodiester between $A_{-1}$ and $G_{+1}$. Transcripts were synthesized in which the body of the tRNA contained either exclusively GMP or exclusively GMPαS. Following cleavage of these substrates with RNase P, the

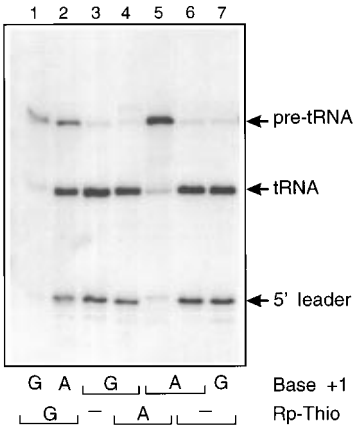


FIGURE 4: Processing of thio-substituted wild-type and mutant pre-$tRNA^{Phe}$ by RNase P RNA subunit in 10 mM $MgCl_2$. Wild-type yeast pre-$G_1$Phe (lanes 1, 3, 4, and 7) and the variant pre-$A_1$Phe (lanes 2, 5, and 6) were synthesized either with phosphate-containing nucleotides (lanes 3, 6, and 7) or with 100% substitution by either GMPαS (lanes 1 and 2) or AMPαS (lanes 4 and 5). tRNA precursors (70−100 nM) were processed for 7 h at 37 °C with 700 nM *E. coli* RNase P RNA in 20 μL of 50 mM Tris-HCl (pH 8.0), 1 M $NH_4Cl$, and 10 mM $MgCl_2$.

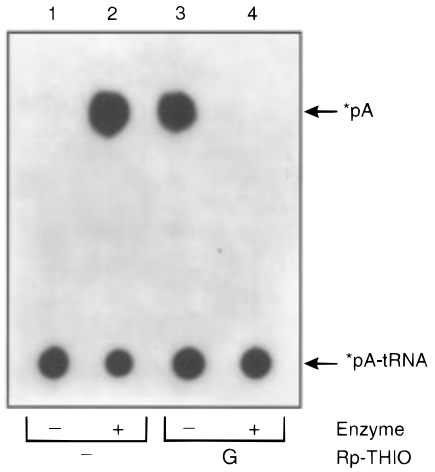


FIGURE 5: Processing of dinucleotide-primed [5′-$^{32}$P]pA-tRNA transcripts. Precursor [5′-$^{32}$P]pA-tRNA (2−10 nM), unsubstituted (lanes 1 and 2) or fully substituted with GMPαS (lanes 3 and 4), was processed with 50 nM *E. coli* RNase P RNA in 10 μL of 50 mM Tris-HCl (pH 8.0), 100 mM $NH_4Cl$, and 60 mM $MgCl_2$ at 37 °C for 30 min. The released product was analyzed by PEI−cellulose thin-layer chromatography using the Li−formate system (see Methods). The positions of unreacted substrate at the origin and of the internal marker 5′-AMP are indicated. In this TLC system, $P_i$ migrates between the origin and pA.

released 5′ leader was detected by thin-layer chromatography. Figure 5 shows that both *pA-tRNA[GMP] (lane 2) and *pA-tRNA[GMPαS] (lane 3) released comparable amounts of *pA after incubation with RNase P RNA. GMPαS-substituted *pA-tRNA was therefore cleaved efficiently and at the same site as the unsubstituted substrate, demonstrating that phosphorothiolation 5′ to guanosine residues other than at the scissile bond does not significantly affect the RNase P reaction.

Together, the data of Figures 3−5 clearly demonstrate that uniform substitution of pre-$tRNA^{Phe}$ with either AMPαS or GMPαS does not significantly inhibit processing by RNase P RNA unless the substitution occurs at the scissile bond itself. The scissile bond is thus the sole position at which introduction of an $R_P$ sulfur is sufficient to prevent cleavage by the catalytic RNA subunit of *E. coli* RNase P.

*Manganese-Dependent Restoration of Cleavage at pro-$R_P$ Sulfur-Containing Bonds.* The inhibition of pre-tRNA cleavage resulting from phosphorothioate substitution at the scissile bond could result in principle either from a chemical effect or a metal coordination effect. The chemical effect results from the reduced electronegativity of sulfur versus oxygen. A phosphorothioate phosphorus is consequently less polarized and is a somewhat weaker target for nucleophilic attack than is a phosphate phosphorus. The magnitude of this effect has been found to result in a 1−11-fold reduction in the rate constant for associative hydrolysis of a phosphorothiodiester bond versus a phosphodiester bond (Herschlag et al., 1991). On the other hand, a metal coordination effect results from the decreased affinity of $Mg^{2+}$ for S rather than for O (see Introduction). $Mg^{2+}$ coordinates preferentially to oxygen, whereas softer metals like $Mn^{2+}$, $Zn^{2+}$, or $Cd^{2+}$ can, in increasing order, coordinate better to sulfur. Of these metals, only $Mn^{2+}$ fully supports the RNase P RNA-catalyzed reaction (Smith & Pace, 1993). Unlike a chemical inhibition, a coordination inhibition induced by sulfur substitution can be overcome or rescued by replacement of $Mg^{2+}$ with a softer metal. We can thus distinguish between phosphorothioate inhibition based on chemical reactivity and one based on metal coordination by two simple tests. First, inhibition of metal coordination should be partially reversed or rescued by replacing $Mg^{2+}$ with $Mn^{2+}$. Second, if reactivity is limited by the amount of bound metal, the apparent first-order rate constant for phosphodiester bond hydrolysis should be quantitatively commensurate with the association constants for metal binding to oxygen or sulfur. We tested both of these predictions by qualitative and quantitative assays of *E. coli* RNase P RNA activity against oxygen- or sulfur-containing pre-tRNA in the presence either of $Mg^{2+}$ or $Mn^{2+}$. Reactions were initially performed at concentrations of $NH_4Cl$ (1.0 M) and $MgCl_2$ (10 mM) or $MnCl_2$ (2 mM) which are optimal for multiple-turnover reactions (Smith et al., 1992).

Figure 6 shows the results of a qualitative processing reaction. Unsubstituted pre-$G_1$Phe is processed almost completely (in a 10-fold overdigestion) in buffer containing either 10 mM $MgCl_2$ or 2 mM $MnCl_2$, as seen in lanes 2 and 3 of Figure 6A. Cleavage of the thio-substituted substrate pre-$G_1$Phe[GMPαS] is barely detectable in the presence of 10 mM $MgCl_2$ (lane 4), whereas cleavage is restored to a significant but less-than-control level with only 2 mM $MnCl_2$ (lane 5). To determine whether elevated $Mg^{2+}$ concentrations would also restore cleavage of the thiolated substrate, an identical reaction was performed in 60 mM $Mg^{2+}$. Figure 6B, lane 4, demonstrates that in prolonged reactions with 60 mM $Mg^{2+}$, RNase P cleaved pre-$G_1$Phe[GMPαS] both at the phosphorothioate bond 5′ to nucleotide $G_{+1}$, and to a greater extent at the phosphate-containing bond 5′ to nucleotide $A_{-1}$. The apparent ratio of cleavage at nucleotide −1 to cleavage at +1 is ca. 3:1. Replacement of $Mg^{2+}$ by $Mn^{2+}$ restores cleavage to position +1 exclusively (Figure 6B, lane 5). Similar analysis of pre$A_1$-Phe demonstrated that replacement of AMP by AMPαS, which introduces phosphorothioates 5′ to nucleotides −1 and +1, forces cleavage (in 60 mM $Mg^{2+}$) to occur exclusively at position +2 within the mature tRNA (data

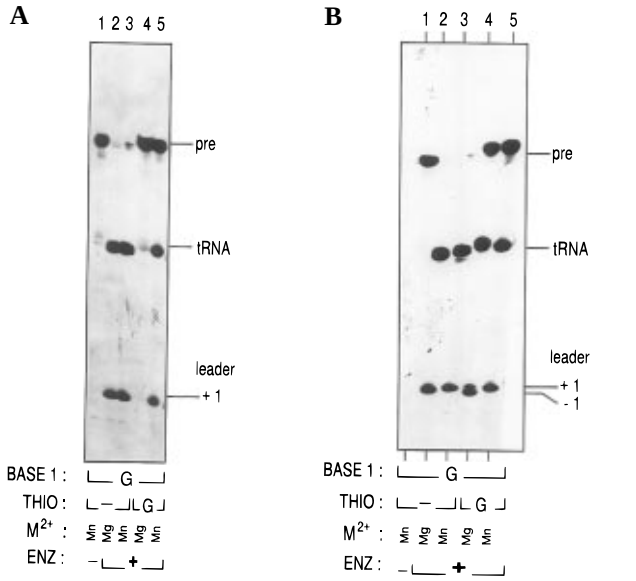


FIGURE 6: Phosphorothioate inhibition and manganese restoration of RNase P cleavage. (A) Ten to 20 nM precursor pre-$G_1$Phe, either unsubstituted (lanes 1−3) or GMPαS-substituted (lanes 4−5), was incubated with buffer only (lane 1) or with 1.5 nM RNase P RNA subunit (lanes 2−5) at 37 °C for 320 min in buffer containing 50 mM Tris-HCl (pH 8.0), 1.0 M $NH_4Cl$, 10 mM DTT, 0.5% SDS, and either 10 mM $MgCl_2$ (lanes 2 and 4) or 2 mM $MnCl_2$ (lanes 1, 3, and 5). (B) Pre-$G_1$Phe (10−20 nM), either unsubstituted (lanes 1−3) or substituted with GMPαS (lanes 4 and 5), was processed with 1.5 nM RNase P RNA (lanes 2−5) in 50 mM Tris-HCl (pH 8.0), 1.0 M $NH_4Cl$, 10 mM DTT, and 0.5% SDS plus either 60 mM $MgCl_2$ or 2 mM $MnCl_2$. Reactions proceeded for 320 min at 37 °C. Products were detected by gel electrophoresis and autoradiography. The two 5′ leader species detected were produced by cleavage 5′ to nucleotides +1 or −1 where +1 is the first nucleotide of mature tRNA.

not shown). Preliminary experiments (not shown) indicated that replacement of Mg by Mn can restore cleavage of $A_1$-Phe[AMPαS] to position +1.

The exact position of RNase P cleavage was confirmed by 5′ end analyses of the products of similar reactions. Pre-tRNAs were internally labeled either with [α-$^{32}$P]CTP so that the 5′ terminus $pG_{+1}p$* or $p(S)G_{+1}p$* would be labeled by nearest-neighbor transfer or with [α-$^{32}$P]ATP to label 5′-termini produced by cleavage at the upstream *$pA_{-1}p$. (The asterisk indicates the labeled phosphate.) tRNA-sized cleavage products were gel-purified and digested to completion with RNase T2. The digestion products, a mixture of internally-derived nucleoside 3′-monophosphates (Np's) and a 5′-terminal nucleoside 5′,3′-bisphosphate (pNp), were separated by chromatography on PEI-cellulose thin-layer plates, as shown in Figure 7. Unsubstituted pre-$G_1$Phe was uniquely cleaved 5′ to $G_{+1}$, generating pGp* 5′-termini, both in 10 mM $MgCl_2$ (Figure 7, lane 2) and in 10 mM $MnCl_2$ (lane 4). No 5′ *pAp termini, the products of cleavage at position −1, could be detected (Figure 7, lanes 1 and 3). Pre-$G_1$Phe labeled with [α-$^{32}$P]ATP and substituted with GMPαS, however, was cleaved in 10 mM $MgCl_2$ predominantly to an alternate product whose 5′ terminus comigrated with pAp (Figure 7, lane 5) and was thus inferred to be *$pA_{-1}p(S)$ or its oxidation product *pAp. Analysis of product labeled with [α-$^{32}$P]CTP demonstrated that a much lower extent of cleavage occurred 5′ to $G_{+1}$, producing 5′-terminal p(S)Gp* and its oxidation product pGp* (Figure 7, lane 6). In the presence of 10 mM $MnCl_2$, however, cleavage of pre-$G_1$Phe[GMPαS] was restored to the correct position, $G_{+1}$, producing tRNA containing exclusively the 5′ terminus

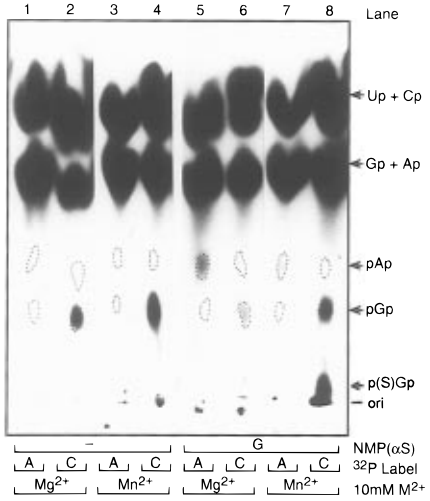


FIGURE 7: Metal-dependent selection of RNase P cleavage site in oxygen and thio-containing pre-tRNAs. Mature-sized tRNAs from experiments like those shown in Figure 6 were gel-purified and subjected to 5′-mononucleotide analysis after digestion with RNase T2. The substrate was pre-G1Phe containing either the four unmodified nucleotides (lanes 1−4) or 100% replacement with GMPaS (lanes 5−8). In lanes 1, 3, 5, and 7, the labeled nucleotide was [α-$^{32}$P]ATP and the nucleotide at position −1, whereas in lanes 2, 4, 6, and 8 it was [α-$^{32}$P]CTP and the 3′ nearest neighbor to nucleotide $G_{+1}$. RNase P RNA cleavage reactions were performed in buffer containing 10 mM $MgCl_2$ (lanes 1, 2, 5, and 6) or 10 mM $MnCl_2$ (lanes 3, 4, 7, and 8). RNase T2 digestion products were separated on PEI−cellulose TLC plates developed with 1.6 M LiCl. The chromatographic origin is indicated by the solid line at the right, and the positions of internal marker nucleotides pAp and pGp are outlined. The product pAp(S) (lane 5) is expected to comigrate with pAp based on control analyses (not shown), indicating that pGp(S) comigrates with pGp. In the analyses shown in lanes 6 and 8, pGp arose by oxidation of p(S)Gp during sample workup and chromatography. Evidence for the identity of p(S)Gp is discussed in the text.

p(S)Gp* (Figure 7, lane 8). Virtually no cleavage at position −1 (giving rise to pAp) was detected (lane 7).

The stability of nucleotide phosphorothioates under our analytical conditions is illustrated by examination of lane 8 of Figure 7. The migration position of p(S)Gp*, near the chromatographic origin, was determined both by TLC analysis of chemically-synthesized p(S)Gp and, in analyses of material from other reactions, by demonstration that iodine cleavage released Gp* (B. C. Thomas and P. Gegenheimer, manuscript in preparation). In most experiments, 20−50% of the starting [3′-$^{32}$P]p(S)Gp* was oxidized to [3′-$^{32}$P]pGp* prior to or during the thin-layer analysis. This oxidation is probably enhanced by electrophilic catalysis by the imino groups of the PEI−cellulose thin-layer plates, as described by Frey (1989, p 147). The pGp product in lanes 6 and 8 of Figure 7 did not originate from GTP contamination in the GTPαS used for transcription because (i) the amount of pGp detected was substantially greater than the manufacturer's measured contamination (about 1%) of GTPαS by GTP and (ii) the ratio of 5′-terminal pGp to p(S)Gp is relatively constant regardless of whether the RNase P reaction is performed with $Mg^{2+}$ or $Mn^{2+}$.

*Quantitative Measurement of the "Thio Effect" and Its Reversal by $Mn^{2+}$.* The relative association constants of $Mg^{2+}$ or $Mn^{2+}$ bound to βO or βS atoms in ATP and ATPβS have been calculated (see Introduction). $Mg^{2+}$ has a 31000-fold lower affinity for S than for O. In contrast, $Mn^{2+}$ coordinates sulfur at the β phosphorus of ATP some 177-fold better than does $Mg^{2+}$, although still roughly 175-fold

weaker than it coordinates a $\beta$ oxygen. The affinities of these ions to the *pro-*$R_P$ oxygen or $R_P$ sulfur of polynucleotides are likely to be similar to their affinities for nucleotide $\beta$-phosphoryls (see Discussion). If a directly-coordinated metal is required for RNase P catalysis, then replacement of the *pro-*$R_P$ oxygen by sulfur will reduce the rate constant for catalysis by a factor close to the decrease in binding of $Mg^{2+}$ to sulfur.

Determination of $k_{chem}$ is complicated by the fact that under steady-state conditions product release is the rate-limiting step of the reaction catalyzed by the RNA subunit alone (Reich et al., 1988; Tallsjö & Kirsebom, 1993; Beebe & Fierke, 1994), and the steady-state parameter $k_{cat}$ is limited by, and numerically close to, $k_{off}$ (Smith et al., 1992; Beebe & Fierke, 1994). To measure $k_{chem}$, we therefore performed single-turnover reactions in which the E·S complex was formed by mixing a saturating excess of RNase P RNA with substrate RNA. Decay of the E·S complex was measured by quenching aliquots of the reaction mixture in 10 M urea at 65 °C. Because cleavage of unsubstituted substrate at pH 8.0 is too rapid to be measured manually and because 10 mM $Mn^{2+}$ approaches insolubility at pH 8 (Dahm et al., 1993; Pan et al., 1993), we performed most reactions at pH 6.0. Cleavage of pre-$G_1$Phe[GMP$\alpha$S] in the presence of 10 mM $Mg^{2+}$ was so slow as to be undetectable at pH 6 and was therefore measured at pH 8; rate constants at pH 8 were extrapolated to pH 6 using a linear dependence of hydrolysis on $[OH^-]$ (Smith & Pace, 1993).

The standard assay measures decay of substrate from the E·S complex. However, for substrate pre$G_1$-Phe[GMP$\alpha$S], cleavage in the presence of $Mg^{2+}$ occurs at two sites, only one of which is the correct one, 5′ to nucleotide +1 (e.g. Figure 6B, lane 4). To estimate the rate of hydrolysis at the correct bond alone, we estimated the rates and extents of cleavage at nucleotides +1 and −1 from a few single-turnover reactions in which the two 5′ leader RNAs could be separated from each other well enough for quantitation. In such a reaction conducted in the presence of 100 mM $Mg^{2+}$, the measured rate and extent of cleavage were roughly equal, the ratio of $k_{obs}$ being 1.2:1 and the ratio of maximum product formed being 1.3:1, for cleavage at nucleotide +1 versus cleavage at −1 (data not shown). For several reactions conducted in 10 mM $MgCl_2$ (in which separate rates were not measured) the amount of products produced by cleavage at the two positions was very nearly identical, although in a few reactions the ratio appeared to favor cleavage at position −1 by 2:1 or 3:1.

For comparison to published values, kinetic measurements were first performed on the unsubstituted wild-type pre-tRNA$^{Phe}$ at a $MgCl_2$ concentration (100 mM) which is close to saturating for $k_{chem}$. The results of a typical analysis are shown in Figure 8. Since the data illustrated displayed a clear lag prior to cleavage, they were fit by a model of sequential binding followed by cleavage as described in Methods. The value of $k_{obs}$ determined at pH 6.0 was (4.13 ± 0.22) × $10^{-2}$ $s^{-1}$. Extrapolation to pH 8.0 gives $k_{obs}$ = 4.1 ± 0.2 $s^{-1}$, which corresponds well with $k_{chem}$= 5.9 ± 0.3 $s^{-1}$ determined directly at pH 8.0 using rapid stop−quench kinetics (Beebe & Fierke, 1994). Moreover, the calculated association rate constant for enzyme−substrate binding ($k_1$) was (3.63 ± 1.00) × $10^6$ $M^{-1}$ $s^{-1}$, within the range of 3 to 6 × $10^6$ $M^{-1}$ $s^{-1}$ obtained for *B. subtilis* RNase P RNA by Beebe and Fierke (1994).

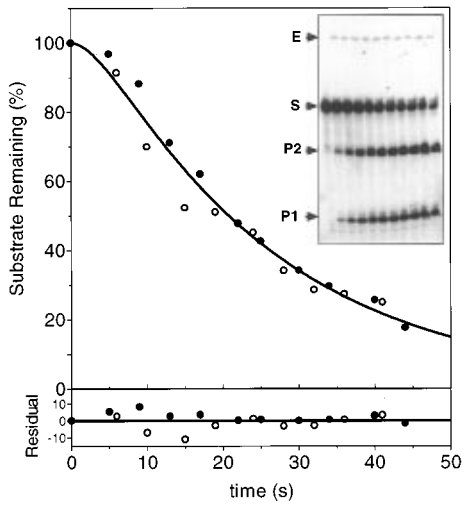


FIGURE 8: Single-turnover kinetic analysis of wild-type substrate. Pre-tRNA$^{Phe}$ (pre-$G_1$Phe), containing all phosphate nucleotides, was reacted with excess RNase P RNA (73 nM) at pH 6.0 and 100 mM $MgCl_2$ as described in Methods. The fraction of substrate remaining was fitted to the sequential binding and cleavage equation described in Methods. The residuals from this estimating equation are plotted in the lower panel. Open and closed symbols represent duplicate assays conducted in parallel. The inset shows the autoradiograph of electrophoretically-separated substrate and products for one of the duplicate reactions. Electrophoretic positions are labeled for E, enzyme RNA; S, substrate; P2, mature tRNA; and P1, 5′ leader RNA.

Further reactions were performed at 10 mM $Mg^{2+}$ or $Mn^{2+}$. Ten millimolar $Mg^{2+}$ is close to optimal for the steady-state reaction (Smith et al., 1992) and for the cooperative phase of the single-turnover reaction (Smith & Pace, 1993), yet, unlike higher concentrations of $Mg^{2+}$, does not support excessive cleavage at alternate sites (compare Figure 6A to Figure 6B). We also found 10 mM $Mn^{2+}$ to be optimal for multiple-turnover reactions (not shown). The results of these kinetic experiments are presented in Figure 9. A summary of $k_{obs}$ determinations for hydrolysis of oxygen- or sulfur-containing pre-tRNA$^{Phe}$ in the presence of $Mg^{2+}$ or $Mn^{2+}$ is presented in Table 1A, and a comparison of $k_{obs}$ with metal affinities for oxygen and sulfur is given in Table 1B. Replacement of the scissile *pro-*$R_P$ oxygen by sulfur reduces the apparent rate constant for magnesium-dependent pre-tRNA hydrolysis, $k_{obs}^{Mg}$, by 28400-fold. This decrease is commensurate with the 31000-fold reduced affinity of $Mg^{2+}$ for $\beta$S versus $\beta$O in ATP. In the presence of $Mn^{2+}$, however, the replacement of oxygen by sulfur reduces $k_{obs}^{Mg}$ only by 77-fold, again commensurate with the ~175-fold reduction in the affinity of $Mn^{2+}$ for S compared with $Mn^{2+}$ for O. As seen in Table 1C, replacing $Mg^{2+}$ with $Mn^{2+}$ thus rescued or increased $k_{obs}$ for hydrolysis of $R_P$-thio-containing pre-tRNA by 2380-fold. This $Mn^{2+}$-dependent rate is still 12-fold lower than the rate for $Mg^{2+}$-promoted cleavage of the oxygen-containing substrate. From these data we also note that the rate constant for $Mn^{2+}$-dependent hydrolysis of the all-oxygen-containing substrate is 6.4-fold greater than the rate constant for $Mg^{2+}$-dependent hydrolysis. This increase is consistent with several roles for $Mg^{2+}$ or $Mn^{2+}$ in the hydrolysis step, as will be discussed subsequently. The magnitude of the "Mn rescue" (ca. 2400-fold) is in fact comparable to that of the product (1120-fold)

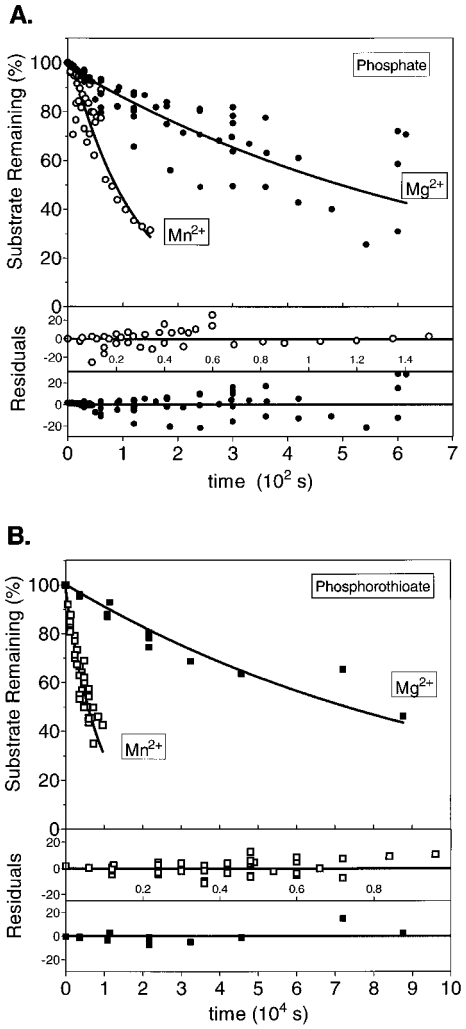


FIGURE 9: Single-turnover kinetics of oxygen or thio-containing substrates catalyzed by $Mg^{2+}$ or $Mn^{2+}$. Data were obtained and analyzed as described in Methods and the legend to Figure 8. For both A and B, the upper panel shows the primary data and computer-fitted curve; the center and bottom panels show the plots of residuals for Mn- and Mg-dependent reactions, respectively. Note that residuals for the Mn-dependent reactions are plotted with expanded x-axes. (A) Cleavage of all-phosphate pre-tRNA. Open circles represent reaction in the presence of 10 mM $MgCl_2$. Data are fit by the single-exponential decay model. Filled circles represent reaction in the presence of 10 mM $MnCl_2$. Data are fit by the sequential binding and cleavage model. (B) Cleavage of GMPαS-containing substrate. Open and filled squares represent reaction in the presence of 10 mM $MgCl_2$ and 10 mM $MnCl_2$, respectively. Both data sets are fit by the single-exponential decay model.

of a 177-fold greater affinity of $Mn^{2+}$ over $Mg^{2+}$ for sulfur and the 6.3-fold greater acidity of Mn hydrate over Mg hydrate.

## DISCUSSION

*$Mg^{2+}$ Coordination by the Scissile Bond.* The simplest explanation of these experimental results is that the magnitude of $k_{obs}$ is governed directly by the affinity of $Mg^{2+}$ or $Mn^{2+}$ for the *pro-*$R_P$ atom of the scissile bond. This interpretation hinges upon knowing first whether the binding of divalent cations in the RNase P enzyme·substrate active site is comparable to their affinity for the $\beta$ phosphate of ATP calculated by Pecoraro et al. (1984) and second whether $k_{obs}$ measures the rate-limiting step in the hydrolysis reaction.

We must first know that the estimated affinities of $Mg^{2+}$ and $Mn^{2+}$ for phosphates in ATP are similar to their affinity

Table 1

A. Single-Turnover Rate Constants for the Thio-Inhibited and Mn-Rescued RNase P reactions[a]

| divalent cation | $R_P$ atom O | $R_P$ atom S |
|---|---|---|
| Mg | $(1.36 \pm 0.08) \times 10^{-3}$ (11) | $(9.57 \pm 0.43) \times 10^{-8}$ [b] (4) |
| Mn | $(8.73 \pm 0.56) \times 10^{-3}$ (4) | $(1.14 \pm 0.06) \times 10^{-4}$ (6) |

B. Thio Inhibition Ratios at Phosphodiester Bond +1

| ligand | $k_{obs}^O/k_{obs}^S$ (experimental)[c] | $K_A^O/K_A^S$ (literature)[d] |
|---|---|---|
| Mg | 28 400 ± 2040 | 31 000 |
| Mn | 77 ± 6 | 175 |
| (Mg:O/Mg:S)/(Mn:O/Mn:S) | 370 ± 28 | 177 |

C. Observed and Expected Manganese Rescue Effect

| ligand | Mn rescue ratio, $k_{obs}^{Mn}/k_{obs}^{Mg}$ experimental[e] | expected | difference |
|---|---|---|---|
| O | 6.42 ± 0 | 6.31[f] | 1.06× |
| S | 2380 ± 160 | 1120[g] | 2.12× |

[a] Numbers are $k_{obs} \pm 1$ SE (standard error of the estimate), in units of $s^{-1}$. In parentheses is the number of replicate determinations pooled in the curve fitting. Data were fitted by the single-exponential decay equation, except for the Mn:O combination which showed a lag and was fitted by the sequential binding and hydrolysis equation. [b] Using $k_{obs}^S$ (phosphate$_{+1}$) = 0.5 × $k_{obs}^S$ (phosphate$_{+1}$ and phosphate$_{-1}$) and corrected from pH 8.0 to pH 6.0; see text. [c] Ratios are calculated from the values of part A and are given ±1 SE. [d] Pecoraro et al. (1984). The entry 175 is the average of 158 and 193; the entry 177 is 31000/175. [e] Calculated from the data of part A. Values are given ±1 SE. [f] Antilog($pK_a^{Mn} - pK_a^{Mg}$); i.e. $K_a^{Mn}/K_a^{Mg}$. [g] Calculated as the expected Mn/Mg binding affinity ratio (177, from part B) times the $K_a$ ratio (6.31).

for phosphates in RNA, and this is likely to be true. For example, the $K_D$ of Mg·ATP, an approximately 60% tridentate complex, is 20 $\mu$M and that of Mg·ADP, a largely bidentate complex, is 78 $\mu$M (Pecoraro et al., 1984). For comparison, $K_D$s of $Mg^{2+}$ for multiple-ligand, high-affinity sites in tRNA range from 10 to 100 $\mu$M (Pan et al., 1993).

Next, which step(s) in the cleavage reaction requires bound $Mg^{2+}$? This, in turn, can be broken down into two questions: (i) Is the rate-limiting step the same for the four different combinations tested of divalent cation and *pro-*$R_P$ atom? (ii) Is the $Mg^{2+}$-dependent step we detect indeed the actual hydrolytic event, or is it an earlier step in the RNase P reaction? In the most general enzyme reaction sequence, formation of the initial enzyme·substrate "collision complex" is followed by conversion to the active or "specific complex" [see Gutfreund (1995), p 186]. For example, a conformational change comparable to "docking" of H-bonded substrate into the catalytic site of the *Tetrahymena* group I intron [e.g. Herschlag and Khosla (1994)], is plausible for many nucleic acid processing enzymes. Additionally, Beebe and Fierke (1994) have identified two kinetic isomers of *B. subtilis* RNase P, differing in their pre-tRNA-binding properties, which must interconvert prior to catalysis.

We can address these questions in turn. First, the consistency of the magnitude of the correlation between our experimental $k_{obs}$ and the predicted $K_D$ for all combinations of divalent cation and *pro-*$R_P$ atom, over a $10^4$-fold range of $k_{obs}$ values, supports the proposal that the same metal-binding event is rate-limiting under all four conditions. Were a rate-limiting conformational change to exist, with a rate constant slower (by definition) than hydrolysis of all-oxygen substrate

but faster than hydrolysis of phosphorothioate substrate, then in changing from oxygen- to sulfur-containing substrate, the change in the rate constants for the limiting steps (isomerization and metal-binding, respectively) would be less than the change in affinity of $Mg^{2+}$ for oxygen versus sulfur. Moreover, if a metal-independent step prior to hydrolysis were rate-limiting, it is unlikely that we could detect the observed increase in $k_{obs}$ for cleavage of oxygen-containing substrate when $Mn^{2+}$ replaces $Mg^{2+}$.

Second, several lines of evidence indicate that we are measuring the rate constant for the chemical step. (i) The value we measure for $k_{obs}$ is consistent with that of $k_{chem}$ determined by other researchers (Smith & Pace, 1993; Beebe & Fierke, 1994). (ii) There is no kinetic evidence for a rate-limiting step between substrate binding and catalysis in single-turnover reactions (Beebe & Fierke, 1994). Although RNase P RNA might exist in two conformers, the kinetic isomerization detected for *B. subtilis* RNase P RNA occurs only after substrate cleavage and so is not rate-limiting in single-turnover reactions. (iii) $k_{obs}$ for cleavage of oxygen-containing substrate increases when $Mg^{2+}$ is replaced by $Mn^{2+}$. This stimulation of activity by $Mn^{2+}$ is consistent with a mechanism involving deprotonation of $Mg{\cdot}OH_2$ or $Mn{\cdot}OH_2$, as discussed below. If the increase in $k_{obs}$ results from the increased acidity of a metal-bound water, then $k_{obs}$ indeed measures the catalytic step. Ultimately, then, the simplest conclusion is that the rate-limiting step in phosphodiester bond hydrolysis requires inner-sphere coordination of $Mg^{2+}$ or $Mn^{2+}$ by the *pro-*$R_P$ nonbridging position of the scissile bond.

*Does the pro-*$R_P$*-bound Cation Also Coordinate the Nucleophilic Water?* Any divalent cation bound to a nonbridging phosphate oxygen is also a candidate for a Lewis acid catalyst which deprotonates water to provide an attacking nucleophile. Our data are completely consistent with a model in which the attacking hydroxide is an inner-sphere ligand to the $Mg^{2+}$ or $Mn^{2+}$ bound to the *pro-*$R_P$ oxygen of the scissile bond. First, the 6.4-fold increase in $k_{obs}{}^{Mn}$ over $k_{obs}{}^{Mg}$ is commensurate with the 6.3-fold increased acidity of $H_2O$ bound to $Mn^{2+}$ rather than to $Mg^{2+}$. [The p$K_a$ of water decreases by 0.8 pH unit when coordinated to $Mn^{2+}$ rather than to $Mg^{2+}$ (Burgess, 1988; Pan et al., 1993).] Second, a supporting line of evidence comes from early observations of Guerrier-Takada et al. (1986), who found that *E. coli* RNase P activity in the presence of $Mg^{2+}$ increased roughly linearly with $[OH^-]$ between pH 4.5 and 6. At or below pH 6, product release is not rate-limiting for catalysis (Smith & Pace, 1993), so that if $K_M$ is constant, overall activity ($\sim k_{cat}/K_M$) is an adequate measure of $k_{chem}$. When the pH dependence of RNase P was determined in the presence of $Mn^{2+}$, a similar dependence was observed but was shifted downward by about 0.5 pH unit (Guerrier-Takada et al., 1986). These data are consistent with deprotonation of water by $Mg^{2+}$ or $Mn^{2+}$ ion in the RNase P reaction.

A note of caution must be raised. We cannot determine, from our data, what fraction of the Mn-dependent increase in $k_{obs}$ might result from increased acidity of a $Mn^{2+}$-bound water molecule and what fraction might result from an increased affinity of $Mn^{2+}$ over $Mg^{2+}$ for phosphate oxygen. Sigel and co-workers (Massoud & Sigel, 1988; Massoud & Sigel, 1989) determined stability constants for monodentate coordination of $Mg^{2+}$ and $Mn^{2+}$ to the phosphate oxygens of simple phosphomonoesters, ribose-5-P, and various nucleotide monophosphates; N7 coordination was excluded. In every instance, phosphate coordination by $Mn^{2+}$ was 3.8−4.2-fold tighter than coordination by $Mg^{2+}$. These data were obtained with free compounds in solution, however, and might not be indicative of relative affinities in the RNase P enzyme·substrate complex.

Taken together, our data are consistent with a proposal that the *pro-*$R_P$-bound $Mg^{2+}$ or $Mn^{2+}$ generates the attacking hydroxide by acidifying a coordinated water molecule. We cannot exclude that some or most of the increased reactivity of $Mn^{2+}$ might result from tighter binding of $Mn^{2+}$ to phosphate oxygens.

*Lack of a Substantial Chemical Effect.* The numerical discrepancy between the magnitude of thio inhibition and manganese rescue effects calculated solely from coordination effects, and their experimentally-observed magnitudes, should be attributable to the intrinsic chemical thio effect described earlier. Since $k_{obs} = k_{chem}K_A{}^{Mg}[Mg^{2+}]$, the chemical thio effect, $k_{chem}{}^O/k_{chem}{}^S$, equals $(k_{obs}{}^O/k_{obs}{}^S)/(K_A{}^{Mg:O}/K_A{}^{Mg:S})$, which is (28400 ± 2040)/31000 or 0.92 ± 0.07. In other words, there is no measurable chemical thio effect within the error of these determinations: the entire change in $k_{obs}$ appears to result from changes in metal coordination. A similar lack of chemical thio effect was determined by Herschlag et al. (1991) for intramolecular cleavage (base-catalyzed phosphoryltransfer) of oligonucleotides containing a single $R_P$-phosphorothioate bond. Chemical thio effects on intermolecular phosphodiester cleavage reactions range from 2- to 10-fold (Herschlag et al., 1991, and references cited therein). The chemical thio effect on the RNase P reaction is thus at the low end of those observed for associative phosphodiester cleavage reactions and is consistent with the proposed hydrolytic reaction mechanism.

*A Proposal for the Scissile Bond in the RNase P Active Site.* From the experimental data, it is now possible to propose a detailed model of the scissile bond during RNase P catalysis. Our model, presented in Figure 10, is based on direct or inner-sphere coordination by the *pro-*$R_P$ oxygen of the scissile bond, as shown in this work. We also incorporate three hypothetical features which are consistent with available experimental data and which could define the position of a reactive $Mg^{2+}$ ion: first, indirect or outer-sphere coordination by hydrogen bonding between an inner-sphere water and the 2′-hydroxyl of the nucleotide at position −1 [as suggested by Smith and Pace (1993)], second, outer-sphere hydrogen bonding to N7 of the purine nucleotide at tRNA position +1 [consistent with results reported by Kahle et al. (1990)], and third, activation of the nucleophilic hydroxide ion (Guerrier-Takada et al., 1986).

*Coordination by the pro-*$R_P$ *Nonbridging Oxygen.* Although there are, in principle, many locations for a magnesium ion bound to the *pro-*$R_P$ oxygen, we chose to position this $Mg^{2+}$ at a location we denote as site C, analogous to the position of the hydroxyl moiety of Tyr497 in the crystal structure of Pol I Exo (Beese & Steitz, 1991), because hand- and computer-built models indicate that this position is favorable for direct coordination of the attacking nucleophile. As a consequence of this positioning, we noted that a fully-hydrated magnesium would be in a favorable position to form H-bonds with the upstream 2′-OH and with the downstream N7. The present model (Figure 10) is one which satisfies these bonding possibilities and requires the least movement from the nucleotide conformation of helical domains in the

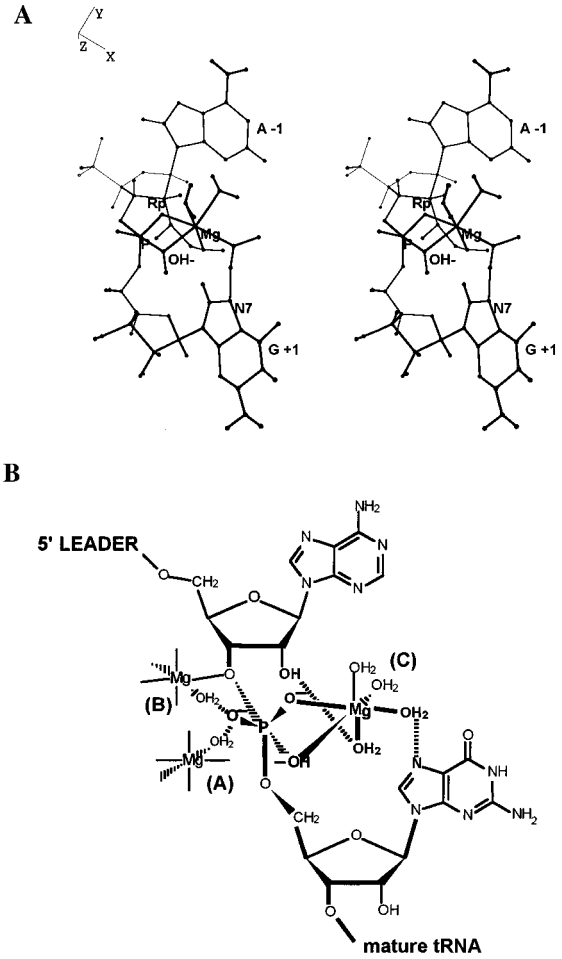


FIGURE 10: A revised model of the scissile bond during the RNase P reaction. These models depict the proposed transition state in phosphodiester bond hydrolysis. (A) Relaxed stereoview of a model built from nucleotide X-ray coordinates as in Methods. The scissile bond is between nucleotides $A_{-1}$ and $G_{+1}$. Labels mark the *pro*-$S_P$ oxygen, attacking $OH^-$, catalytic $Mg(H_2O)_5$, and N7 of $G_{+1}$. (B) Interpretive sketch of the model in panel A. Two additional Mg hydrates are included at sites A and B. The upstream 2′-OH and downstream N7 are marked with bold type.

refined crystal structure of yeast $tRNA^{Phe}$ (Sussman et al., 1978).

Previous models of the RNase P catalytic center (see Figure 1) have presented the opposite stereochemistry at the scissile bond: a $Mg^{2+}$ generating the nucleophilic water was arbitrarily chosen to coordinate the *pro*-$S_P$ rather than the *pro*-$R_P$ oxygen (Haydock & Allen, 1985; Guerrier-Takada et al., 1986; Smith & Pace, 1993), although Smith (1995) has revised that model to indicate *pro*-$R_P$ coordination. Our model also differs from earlier proposals in that we demonstrate that the attacking hydroxide can be an inner-sphere rather than an outer-sphere ligand to the active $Mg^{2+}$.

We show two additional hydrated $Mg^{2+}$ ions occupying sites A and B with indirect (outer-sphere) coordination by the *pro*-$S_P$ oxygen of the scissile bond and direct coordination by O3′. Although the location of these cations is strictly speculative, their presence is suggested by experimental evidence and by comparison with information on the active site of the *T. thermophila* group I intron. At least three $Mg^{2+}$ ions, or classes of ions, are likely to be directly involved in catalysis by RNase P (Smith & Pace, 1993; Beebe et al., 1996), and two of these ions appear to stabilize the E·S complex (Hardt et al., 1993; Beebe et al., 1996). By analogy with the *Tetrahymena* group I intron, one of these ions may directly coordinate O3′ (Piccirilli et al., 1993). Second, catalysis by *E. coli* RNase P RNA is inhibited by thio substitution of the *pro*-$S_P$ oxygen, the magnitude of $k_{obs}$ reduction being severalfold greater than that for thio substitution at the *pro*-$R_P$ position (L. Li and P. Gegenheimer, manuscript in preparation). Furthermore, the lack of $Mn^{2+}$ rescue at the *pro*-$S_P$ position indicates that any essential ligand located there is not directly coordinated

*Outer-Sphere Coordination of pro-$R_P$-bound Magnesium.* Our model indicates that a hydrated magnesium ion is capable of binding simultaneously to three ligands surrounding the scissile bond. For comparison, the $Mg^{2+}$ ion occupying site 1 in the orthorhombic crystal of $tRNA^{Phe}$ (6TNA; Holbrook et al., 1977) has one inner-sphere and five outer-sphere ligands to tRNA; this is presumed to correspond to a tight-binding site. Indeed, indirect evidence is consistent with multiple ligands to the *pro*-$R_P$-bound Mg in the RNase P reaction.

The ribose 2′-hydroxyl of pre-tRNA nucleotide −1 has already been implicated in formation of a binding site for a catalytically-involved magnesium ion. Removal of this 2′-OH reduces $k_{obs}$ 3400-fold and reduces the cooperativity of $Mg^{2+}$ binding from 3 to 2 [Smith & Pace, 1993; Perreault and Altman (1992) and Kleineidam et al. (1993) present comparable data although $k_{obs}$ was not determined]. Moreover, replacement of this 2′-OH with 2′-OMe reduces $k_{obs}$ $\sim 10^6$-fold. This evidence implicates the upstream 2′-OH in stabilizing a hydrated magnesium ion, most likely by serving as an H-bond donor to an inner-sphere water (Smith & Pace, 1993).

Another potential ligand to a hydrated divalent cation is N7 of the purine ring 3′ to the scissile bond. In the orthorhombic crystal structure of $tRNA^{Phe}$ (6TNA), the $Mg^{2+}$ at "site 1", which is directly coordinated by the *pro*-$S_P$ phosphodiester oxygen of G19, is indirectly coordinated via outer-sphere hydrogen bonding to N7 of the downstream G20. Furthermore, in the complex of $Mg^{2+}$ with 5′-AMP, up to 5−10% of the bound hydrated $Mg^{2+}$ forms a macrochelate in which an outer-sphere water coordinates adenine N7 (Massoud & Sigel, 1989). For the $Mn^{2+}$·5′-AMP complex, approximately 15% of the metal is coordinated directly or indirectly to N7 (Massoud & Sigel, 1989) and perhaps half of that is in indirect (outer-sphere) macrochelates [see Sigel (1987) for macrochelate formation with ATP]. These data indicate that a binding site for the *pro*-$R_P$ phosphate-bound $Mg^{2+}$ could be completed by outer-sphere coordination from N7 of the purine at position +1. This possibility is reinforced by the demonstration that methylation of N7 in pre-tRNA completely prevents pre-tRNA cleavage by the RNA subunit of *E. coli* RNase P (Kahle et al., 1990). Control experiments showed that $G_{+1}$ was the only position at which N7 methylation blocked cleavage. Enzyme in 10-fold excess over that required to produce 100% cleavage of unmodified substrate released no detectable product from $m^7$G-substituted pre-tRNA [Figure 2 in Kahle et al. (1990)]. The severity of inhibition suggests a 100−1000-fold decrease in $k_{cat}$, a magnitude which is consistent with blockage of $Mg^{2+}$ binding.

We emphasize that, although adenosine 2′-hydroxyl and guanine N7 can physically coordinate a *pro*-$R_P$-bound $Mg^{2+}$, there is no experimental evidence that they actually do so

nor that, if they did, they must coordinate the same ligand.

*Participation of Purine N7.* A requirement for $Mg^{2+}$ coordination to N7 of the guanine 3′ to the scissile bond would partly explain the predominance of purines at position +1 of bacterial tRNAs. For example, of 276 (eu) bacterial tRNA sequences in the tRNA sequence database (Steinberg et al., 1993) with 5′ termini at +1, 82% initiate with a purine nucleotide (79% with G and 3% with A), 13% with C, and 5% with U. (Details of this analysis are given in the Methods.) A similar distribution is found for 375 eukaryotic cytoplasmic tRNAs, 82% of which start with a purine (76% G, 6% A), 6% with cytidine, and 12% with uracil. Indeed, of 1759 tRNA sequences from all organisms for which base +1 is the 5′ end, 83% start with purines (67% guanine, 16% adenine) and 17% initiate with pyrimidines (8% cytidine, 9% uracil). This distribution is consistent with a requirement for an H-bond acceptor in the base at position +1. In the purines this acceptor is N7. In the *anti* conformation of the pyrimidine base, uracil O4 and cytidine N4 (as an H-bond donor rather than an acceptor) are poor substitutes for N7, but if the pyrimidine ring were rotated into the less-favored *syn* conformation, N3 would occupy the position of the purine N7.

*Role of the Enzyme RNA in Metal Coordination.* The site specificity of RNase P cleavage implies that $Mg^{2+}$ ion(s) at the substrate's scissile bond are likely to be coordinated by specific ligands provided by the active site of the enzyme. Examination of molecular models of the enzyme·substrate complex (Harris et al., 1994; Westhof & Altman, 1994) reveals numerous enzyme phosphodiesters which are exposed in the modeled active site and which surround the scissile bond. Direct assay, by phosphorothioate modification interference and manganese rescue, demonstrates that phosphates whose *pro-*$R_P$ oxygens are required for substrate binding or phosphodiester bond hydrolysis are predominantly clustered along the major groove of helix P4 in the *E. coli* RNase P RNA (Harris & Pace, 1995; Hardt et al., 1995). In particular, U69 and possibly C70 directly coordinate $Mg^{2+}$ ion(s) required for binding stabilization (Hardt et al., 1995), and the phosphate 5′ to A67 donates its *pro-*$R_P$ oxygen as a ligand to a catalytically-required magnesium ion (Harris & Pace, 1995). Examination of our proposed model for the scissile bond indicates that the binding site for $Mg^{2+}$-C could be formed largely from ligands provided by the substrate; the major role of the enzyme would thus be to bind pre-tRNA in the transition-state conformation depicted in Figure 10. In this structure, the two nucleosides surrounding the scissile bond have been "opened up" to permit facile entry of a hydrated magnesium ion. This conformational rearrangement is consistent with protection mapping data of Knap et al. (1990) which indicate that pre-tRNA substrate partially unfolds upon binding the RNA subunit. We propose that functional groups of the enzyme may be more important in coordinating $Mg^{2+}$ ions bound at sites other than C, perhaps at sites A and B.

*Cleavage Site Selection.* The present data provide a strong indication that the selected scissile bond in a pre-tRNA is that one, closest to the "correct" site, at which a $Mg^{2+}$ (or $Mn^{2+}$) ion can bind the *pro-*$R_P$ phosphate oxygen. Our observation of alternate cleavage sites in phosphorothioate-substituted pre-tRNA is consistent with the proposal that when the correct phosphodiester bond is blocked by the presence of an $R_P$ sulfur atom, RNase P RNA will cleave slowly at the oxygen-containing bond closest to the correct site, with preference for the upstream over the downstream bond. A similar utilization of alternate cleavage sites 5′ to nucleotides −1 or +2, when the correct site (+1) was thiolated, was described by Kahle et al. (1993). Furthermore, Smith and Pace (1993) demonstrated that replacement of the upstream 2′-OH with 2′-OMe forced slow cleavage at nucleotide +2 within the tRNA as well as at the correct site. The slow rate, higher magnesium requirement, and manganese reversal (shown in the present work) of these alternate cleavages suggest that they depend upon $Mg^{2+}$ coordinated to the *pro-*$R_P$ oxygen at secondary, low-affinity sites in the substrate. This implies that a mechanism exists whereby an alternate scissile bond can be placed into the catalytic site or that a catalytic site can be formed at an alternate position. For example, *E. coli* RNase P does possess the intrinsic ability to catalyze hydrolysis of pre-$tRNA^{His}$ substrates at position −1 (Burkard et al., 1988).

Scheme 2

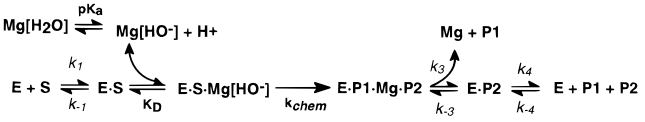


*A Revised Kinetic Description of the RNase P Reaction.* Drawing on the scheme presented in the introduction, details discussed above, and the kinetic steps delineated by Beebe and Fierke (1994), we can now justify a more detailed kinetic model for the RNase P reaction (Scheme 2).

Several features of this scheme are noteworthy. First, we propose that the binding site for the reactive magnesium exists only in the E·S complex when the scissile bond is distorted toward the transition-state conformation. This site, whose existence requires flexing of the scissile bond away from the geometry of A-helical RNA, is unlikely to exist in native pre-tRNA if the base at position −1 is stacked on base 1 or maintains any helical character. Second, the catalytic Mg hydrate binds the E·S complex as $Mg[OH]^-$. Although this is not a necessary feature of the structural or kinetic model, the data are consistent with generation of hydroxide by an aqueous $Mg^{2+}$ ion. (Conceivably, its acidity could increase upon binding the E·S complex.) This feature of the model is consistent with the demonstration that the hydrolysis reaction has a measurable $K_M$ for hydroxide ion (Smith & Pace, 1993); we suggest that this $K_M$ is actually that of the $Mg[HO^-]$ species. [Indeed, Smith and Pace (1993) found $K_M$ for hydroxide to be essentially the same as $K_M$ for $Mg^{2+}$.] Under these circumstances, RNase P reaction velocity will be limited by the concentration of $Mg[HO^-]$, or in other words, $k_{obs}$ in our experiments is $k_{chem}[Mg{\cdot}OH^-]K_A^{Mg[HO^-]}$. Third, the catalytic $Mg^{2+}$ must dissociate following cleavage—certainly with or before dissociation of the 5′ leader—as its binding site is eliminated by phosphodiester hydrolysis.

In conclusion, localization of the *pro-*$R_P$-bound $Mg^{2+}$ allows construction of several realistic and testable models, one of which we propose in Figure 10, for the scissile bond in the RNase P hydrolysis reaction. The proposed disposition of metal ligands in this RNA-catalyzed reaction is similar to that in some protein-catalyzed phosphodiester bond hydrolysis reactions. Current efforts are directed toward evaluating the involvement of other potential $Mg^{2+}$ ligands by the substrate as well as by the enzyme.

## ACKNOWLEDGMENT

We are grateful to Drs. O. C. Uhlenbeck for providing plasmid p67YF0 and N. R. Pace and D. Waugh for the gift of plasmid pDW27 (*E. coli* RNase P RNA subunit). Dr. T. Steitz generously provided unpublished coordinates of the active site of the exonuclease domain of *E. coli* DNA polymerase I. Dr. S. Altman pointed out, many years ago, the preponderance of guanine as the first base of tRNAs. We benefited from discussions of, and tutelage on, enzyme kinetics and metal coordination with Drs. R. Schowen, R. Himes, and K. Bowman-James and of the interpretation of rate-limiting steps with D. Herschlag.

## REFERENCES

Altman, S. (1989) *Adv. Enzymol. Relat. Areas Mol. Biol. 62*, 1−36.
Altman, S., & Smith, J. D. (1971) *Nature New Biol. 233*, 35−39.
Beebe, J. A., & Fierke, C. A. (1994) *Biochemistry 33*, 10294−10304.
Beebe, J. A., Kurz, J. C., & Fierke, C. A. (1996) *Biochemistry 35*, 10493−10505.
Beese, L. S., & Steitz, T. A. (1993) *EMBO J. 10*, 25−33.
Brown, J. W., & Pace, N. R. (1992) *Nucleic Acids Res. 20*, 1451−1456.
Burgess, J. (1988) *Ions in Solution*, pp 63−67, Ellis Horwood Ltd, Chichester, England.
Burkard, U., Willis, I., & Söll, D. (1988) *J. Biol. Chem. 263*, 2447−2451.
Cedergren, R., Lang, B. F., & Gravel, D. (1987) *FEBS Lett. 226*, 63−66.
Christian, E. L., & Yarus, M. (1993) *Biochemistry 32*, 4475−4480.
Cox, B. G. (1994) *Modern Liquid Phase Kinetics*, pp 26−28, Oxford University Press, New York.
Dahm, S. C., & Uhlenbeck, O. C. (1991) *Biochemistry 30*, 9464−9469.
Dahm, S. C., Derrick, W. B., & Uhlenbeck, O. C. (1993) *Biochemistry 32*, 13040−13045.
Darr, S. C., Brown, J. W., & Pace, N. R. (1992) *Trends Biochem. Sci. 17*, 178−182.
Dunaway-Mariano, D., & Cleland, W. W. (1980) *Biochemistry 19*, 1496−1505.
Eckstein, F. (1985) *Annu. Rev. Biochem. 54*, 367−402.
Fersht, A. (1985) *Enzyme Structure and Mechanism*, 2nd ed., W. H. Freeman, New York.
Frey, P. A. (1989) *Adv. Enzymol. Relat. Areas Mol. Biol. 62*, 119−195.
Frey, P. A., & Sammons, R. D. (1985) *Science 228*, 541−545.
Gardiner, K., & Pace, N. R. (1980) *J. Biol. Chem. 255*, 7507−7509.
Gardiner, K. J., Marsh, T. L., & Pace, N. R. (1985) *J. Biol. Chem. 260*, 5415−5419.
Guerrier-Takada, C., Gardiner, K., Marsh, T., Pace, N., & Altman, S. (1983) *Cell 35*, 849−857.
Guerrier-Takada, C., Haydock, K., Allen, L., & Altman, S. (1986) *Biochemistry 25*, 1509−1515.
Gutfreund, H. (1995) *Kinetics for the Life Sciences*, Cambridge University Press, Cambridge, U.K.
Hardt, W.-D., Schlegl, J., Erdmann, V., & Hartmann, R. (1993) *Nucleic Acids Res. 21*, 3521−3527.
Hardt, W.-D., Warnecke, J. M., Erdmann, V. A., & Hartmann, R. (1995) *EMBO J. 14*, 2935−2944.
Harris, M. E., & Pace, N. R. (1995) *RNA 1*, 210−218.
Harris, M. E., Nolan, J. M., Malhotra, A., Brown, J. W., Harvey, S. C., & Pace, N. R. (1994) *EMBO J. 13*, 3953−3963.
Haydock, K., & Allen, L. C. (1985) *Prog. Clin. Biol. Res. 172A*, 87−98.
Herschlag, D., & Khosla, M. (1994) *Biochemistry 33*, 5291−5297.
Herschlag, D., Piccirilli, J. A., & Cech, T. R. (1991) *Biochemistry 30*, 4844−4854.
Holbrook, S. R., Sussman, J. L., Warrant, R. W., Church, G. M., & Kim, S.-H. (1977) *Nucleic Acids Res. 4*, 2811−2820.
Hough, E., Hansen, L. K., Birknes, B., Jynge, K., Hansen, S., Hordvik, A., Little, C., Dodson, E., & Derewenda, Z. (1989) *Nature 338*, 357−360.
Jaffe, E. K., & Cohn, M. (1978) *Biochemistry 17*, 652−657.
Jaffe, E. K., & Cohn, M. (1979) *J. Biol. Chem. 254*, 10839−10845.
Kahle, D., Wehmeyer, U., Char, S., & Krupp, G. (1990) *Nucleic Acids Res. 18*, 837−844.
Kahle, D., Küst, B., & Krupp, G. (1993) *Biochimie 75*, 955−962.
Kim, E. E., & Wyckoff H. W. (1991) *J. Mol. Biol. 218*, 449−464.
Kleineidam, R. G., Pitulle, C., Sproat, B., & Krupp, G. (1993) *Nucleic Acids Res. 21*, 1097−1101.
Knap, A. K., Wesolowski, D., & Altman, S. (1990) *Biochimie 72*, 779−790.
Marsh, T. L., & Pace, N. R. (1985) *Science 229*, 79−80.
Massoud, S. S., & Sigel, H. (1988) *Inorg. Chem. 27*, 1447−1453.
Massoud, S. S., & Sigel, H. (1989) *Eur. J. Biochem. 179*, 451−458.
Milligan, J. F., & Uhlenbeck, O. C. (1989) *Biochemistry 28*, 2849−2855.
Morales, M. J., Dang, Y. L., Lou, Y. C., Sulo, P., & Martin, N. C. (1992) *Proc. Natl. Acad. Sci. U.S.A. 89*, 9875−9879.
Oommen, A., Li, X., & Gegenheimer, P. (1992) *Mol. Cell. Biol. 12*, 865−875.
Pace, N. R., & Brown, J. W. (1995) *J. Bacteriol. 177*, 1919−1928.
Pan, T. (1995) *Biochemistry 34*, 902−909.
Pan, T., Long, D. M., & Uhlenbeck, O. C. (1993) in *The RNA World* (Gesteland, R. F., Atkins, J. F., Eds.) pp 271−302, Cold Spring Harbor Laboratory Press, Cold Spring Harbor, NY.
Pecoraro, V. L., Hermes, J. D., & Cleland, W. W. (1984) *Biochemistry 23*, 5262−5271.
Perreault, J. P., & Altman, S. (1992) *J. Mol. Biol. 226*, 399−409.
Piccirilli, J. A., Vyle, J. S., Caruthers, M. H., & Cech, T. R. (1993) *Nature 361*, 85−88.
Rajagopal, J., Doudna, J. A., & Szostak, J. W. (1989) *Science 244*, 692−694.
Reich, C., Olsen, G. J., Pace, B., & Pace, N. R. (1988) *Science 239*, 178−181.
Robertson, H. D., Altman, S., & Smith, J. D. (1972) *J. Biol. Chem. 247*, 5243−5251.
Sambrook, J., Fritsch, E. F., & Maniatis, T. (1989) *Molecular Cloning*, 2nd ed., p 1.38, Cold Spring Harbor Laboratory Press, Cold Spring Harbor, NY.
Sampson, J. R., & Uhlenbeck, O. C. (1988) *Proc. Natl. Acad. Sci. U.S.A. 85*, 1033−1037.
Sigel, H. (1987) *Eur. J. Biochem. 165*, 65−72.
Smith, D. (1995) in *The Biological Chemistry of Magnesium* (Cowan, J. A., Ed.) pp 111−135, VCH Publishers, NY.
Smith, D., & Pace, N. R. (1993) *Biochemistry 32*, 5273−5281.
Smith, D., Burgin, A. B., Haas, E. S., & Pace, N. R. (1992) *J. Biol. Chem. 267*, 2429−2436.
Stark, B. C., Kole, R., Bowman, E. J., & Altman, S. (1978) *Proc. Natl. Acad. Sci. U.S.A. 75*, 3717−3721.
Steinberg, S., Misch, A., & Sprinzl, M. (1993) *Nucleic Acids Res. 21*, 3011−3015.
Steitz, T. A., & Steitz, J. A. (1993) *Proc. Natl. Acad. Sci. U.S.A. 90*, 6498−6502.
Surratt, C. K., Carter, B. J., Payne, R. C., & Hecht, S. M. (1990) *J. Biol. Chem. 265*, 22513−22519.
Sussman, J. L., Holbrook, S. R., Warrant, R. W., Church, G. M., & Kim, S.-H. (1978) *J. Mol. Biol. 123*, 631−660.
Tallsjö, A., & Kirsebom, L. A. (1993) *Nucleic Acids Res. 21*, 51−57.
Volbeda, A., Lahm, A., Sakiyama, F., & Suck, D. (1991) *EMBO J. 10*, 1607−1618.
Volckaert, G., & Fiers, W. (1977) *Anal. Biochem. 83*, 222−227.
Wang, M. J., Davis, N. W., & Gegenheimer, P. (1988) *EMBO J. 7*, 1567−1574.
Waugh, D. S., Green, C. J., & Pace, N. R. (1989) *Science 244*, 1569−1571.
Westhof, E., & Altman, S. (1994) *Proc. Natl. Acad. Sci. U.S.A. 91*, 5133−5137.
Zimmerley, S., Drainas, D., Sylvers, L. A., & Söll, D. (1993) *Eur. J. Biochem. 217*, 501−507.

BI9620464